1974

Nonempirical Molecular Orbital Calculations For The Ground And Lower Excited States Of Some Small Polyatomic Molecules

Robert Francis Barr

NONEMPIRICAL MOLECULAR ORBITAL CALCULATIONS FOR THE GROUND AND LOWER EXCITED STATES OF SOME SMALL POLYATOMIC MOLECULES

by

Robert Francis Barr

Department of Chemistry

Submitted in partial fulfillment
of the requirements for the degree of
Doctor of Philosophy

Faculty of Graduate Studies
The University of Western Ontario
London, Ontario

May, 1974

To Catherine

ABSTRACT

The results of nonempirical theoretical studies based on the molecular orbital theory are reported for a number of small polyatomic molecules of chemical interest. The "half-electron" method and the use of ground state orbitals are compared to the Roothaan restricted open-shell method both on a formal basis, and by contrasting the ab initio energies predicted by these schemes for a series of radicals and triplets to test the efficacy of the former two methods in the computation of wavefunctions and energies of open-shell systems. Use of the Roothaan method rather than the half-electron method is found to lead to an average improvement of 4.8 kcal mol^{-1} in the energies of eight radicals, whereas the average improvement for nineteen triplet states is 8.2 kcal mol^{-1}. The predicted equilibrium geometries do not differ appreciably between these two methods. The use of closed-shell eigenvectors leads to large errors in triplet states for which the electron density distributions differ appreciably from those in the ground state.

Ab initio calculations using the STO-3G basis set for two monomeric organoberyllium compounds, $HBeCH_3$ and $Be(CH_3)_2$, indicate that stablization due to hyperconjugation is larger than was previously supposed. Charge distributions suggest that the degree of ionicity of these systems is less than that of the corresponding alkyllithium compounds. The predicted geometry of $HBeCH_3$

agrees well with available experimental data. In addition, the calculated dimerization energy of $HBeCH_3$ of 4.3 kcal mol^{-1} agrees qualitatively with experimental findings for alkylberyllium compounds. In contrast, similar calculations for $HBeNH_2$ indicate a greater degree of ionicity, the presence of strong π bonds, and large dimerization energies for aminoberyllium compounds.

The electronic structure of carbonylnitrenes is investigated on the basis of STO-3G calculations for the S_0 and T_1 states of formylnitrene and carbhydroxynitrene. The S_0-T_1 separation is predicted to be ≈45 kcal mol^{-1} for both molecules, with the triplet state lying lower in energy. In addition, the S_1 state is predicted to lie close in energy to the S_0 state and the involvement of the former state in the photochemistry of carbonylnitrenes is suggested. Calculations using an extended basis set of orbitals predict that oxazirene and formylnitrene are of comparable stability, and that there is only a small energy barrier to their interconversion. The possible role of oxazirenes in the chemistry of carbonylnitrenes is also discussed.

A study of the bonding and energetics in aminonitrenes is presented using H_2NN as the prototype aminonitrene. Complete geometry optimization for both the lowest singlet and triplet states leads to the prediction that the triplet state lies lower in energy, in contrast to indications from experiment. A rationalization

of this discrepancy, based on shortcomings in the theoretical method, is presented. The effect of methyl, fluoro and carbonyl substituents on the charge distribution and upon the singlet-triplet separation is also studied.

The barriers to internal rotation in ethylene and allene have been calculated using a minimal basis set. For ethylene, a barrier height which is in reasonable agreement with the experimental value can be obtained using the STO-3G basis set and simple 2X2 configuration interaction provided that the C-C bond distance is optimized for both the planar and twisted conformations. A similar calculation for allene using an open-shell SCF method predicts a barrier height of 55.5 kcal mol^{-1}, some 17 kcal mol^{-1} lower than the barrier height in ethylene.

A study of the bonding and energetics in ethylenedione, O=C=C=O, is presented. The ground state is predicted to be a linear triplet and is calculated to lie 17 kcal mol^{-1} below the lowest singlet state. Cis bending of the molecule is predicted to result in a change in electron configuration when the OCC angle reaches ≈120°. The new state correlates with the ground state of two C≡O molecules. It is suggested that this distortion is the principal reason for the lack of success in the synthesis of ethylenedione from 1,2-diones.

ACKNOWLEDGEMENTS

Financial support by the National Research Council of Canada through the award of an NRC Postgraduate Scholarship is gratefully acknowledged.

I wish to express my sincere gratitude to Dr. N. Colin Baird for the guidance and direction which he has provided during the course of this research.

To my wife, Catherine I extend my deepest gratitude for the patience and understanding she has shown during the preparation of this thesis and for her perseverance in its typing.

TABLE OF CONTENTS

LIST OF TABLES

LIST OF FIGURES

DEFINITION OF UNITS

For convenience, some units which do not conform to Système International d'Unités (SI) standards have been used in this thesis. Conversion factors for these units are listed below.

$$1 \text{ kcal} = 4.184 \text{ kJ}$$

$$1 \text{ eV} = 1.6021 \times 10^{-22} \text{ kJ}$$

$$1 \text{ a.u.} = 4.359 \times 10^{-21} \text{ kJ}$$

$$1 \text{ Å} = 10^{-10} \text{ m}$$

$$1^{\circ} \text{ (plane angle)} = \pi/180 \text{ rad}$$

CHAPTER I

GENERAL INTRODUCTION

1. Scope of Work

The molecular orbital model had its origins more than forty-five years ago in the work of Hund (1) and Mulliken (2) who developed it to explain diatomic molecule band spectra. Their success in this area, together with the classic work of Lennard-Jones (3) in elucidating the electronic structure of diatomic molecules and that of Huckel (4) in developing methods for treating conjugated organic molecules, are highlights in the evolution of a theory which has become almost universally accepted in the chemical sciences.

It has only been in the last decade - with the advent of modern digital computers and the concurrent development of sophisticated computational methods - that rigorous investigations of electronic structure, in the framework of the molecular orbital method, have become generally possible. Early applications of these procedures (5) to systems which had already been well characterized experimentally indicated that the theory gives reasonable descriptions of a variety of molecular properties. Encouraged by the results of these studies, the subsequent growth in the use of nonempirical ("ab initio") calculations to investigate molecular electronic struc-

ture has been enormous.[1] In addition, many of the recent applications have dealt with properties or processes which are difficult to examine experimentally, such as the structures of reaction intermediates and the paths of chemical reactions.

The contents of this thesis emphasize two aspects of the current effort in nonempirical molecular orbital theory. In Chapter II, two widely used, but approximate computational schemes for the calculation of self consistent field wavefunctions for open-shell systems are compared to a third, more sophisticated method. Such an investigation is required in order to assess the performance of the approximate schemes and to indicate in which circumstances they can be used safely.

Second, in Chapter III, recently developed molecular orbital methods are applied to a number of systems of chemical interest. Of primary concern in the molecules considered are the equilibrium geometries for the ground state (and in some cases, for the lower excited states), the excitation energies, and the energetics of some of the more interesting intramolecular transformations. In addition, the calculated wavefunctions are used to deduce the charge distributions and the types of bonding present

---

[1]For example, the number of papers (per year) reporting nonempirical calculations on polyatomic molecules has risen from less than 20 in 1964 to almost 200 in 1970 (6).

in each state. It is hoped that the results of these calculations will lead to a greater understanding both of the electronic structure of the particular molecules considered and of the chemical processes involved.

2. Details of Calculations

All of the calculations reported herein have been carried out within the framework of the linear combination of atomic orbitals (LCAO), molecular orbital (MO), self consistent field (SCF) theory. In this approximation, the total molecular electronic wavefunction, Ψ, for a system of 2N electrons is taken to be an antisymmetrized product of orthonormal spatial molecular orbitals, ψ_i, and the spin functions α or β. The spatial functions, in turn, are taken to be linear combinations of basis functions ϕ_u:

$$\psi_i = \sum_u c_{iu} \phi_u \qquad \text{I-1}$$

Once these latter functions are specified, the coefficients, c_{iu}, are chosen to minimize the total electronic energy:

$$E_e = \int \Psi^* \hat{H}_e \Psi d\tau \qquad \text{I-2}$$

where $\hat{H}_e$ is the non-relativistic electrostatic Hamiltonian:

$$\hat{H}_e = -\tfrac{1}{2}\sum_i \nabla_i^2 - \sum_i \sum_\alpha (Z_\alpha / r_{i\alpha}) + \sum_{i>j} (1/r_{ij}) \qquad \text{I-3}$$

A general set of equations for the coefficients has been derived by Roothaan for both closed (7) and open (8) shells of electrons. Specifically, the c_{iu} are determined by solving the set of simultaneous homogeneous equations:

$$\sum_\nu F_{\mu\nu} c_{i\nu} = \varepsilon_i \sum_\nu S_{\mu\nu} c_{i\nu} \qquad \text{I-4}$$

where for closed shells:

$$F_{uv} = H_{uv} + \sum_s P_{rs}\{\langle uv|rs\rangle - \tfrac{1}{2}\langle ur|vs\rangle\} \qquad \text{I-5}$$

$$H_{uv} = \int \phi_u(1)\{-\tfrac{1}{2}\nabla_1^2 - \sum_\alpha (Z_\alpha/r_{1\alpha})\}\phi_v(1)\, d\tau(1) \qquad \text{I-6}$$

$$\langle uv|rs\rangle = \int\int \phi_u(1)\phi_v(1)\{1/r_{12}\}\phi_r(2)\phi_s(2)\, d\tau(1)d\tau(2) \qquad \text{I-7}$$

$$P_{rs} = 2\sum_i^N c_{ir}\, c_{is} \qquad \text{I-8}$$

$$S_{uv} = \int \phi_u(1)\phi_v(1)\, d\tau(1) \qquad \text{I-9}$$

A non-trivial solution for the equations I-4 exists only if the secular determinant vanishes:

$$|F_{uv} - \varepsilon S_{uv}| = 0 \qquad \text{I-10}$$

The N lowest roots, ε_i, of the secular determinant represent the energies of the molecular orbitals ψ_i, and for closed shells are approximations to the ionization potentials. The first term in equation I-5, H_{uv} is the matrix element of the one-electron Hamiltonian and includes the kinetic energy of the electrons and the potential due to electron-nucleus attraction. The second term, sometimes abbreviated G_{uv}, contains the potential due to electron-electron repulsion. Since the matrix elements F_{uv} depend on the coefficients, an iterative method of successive approximations to F_{uv} must be adopted and continued until the electronic energy is stationary with respect to a variation in the coefficients. The total mol-

ecular energy is then obtained by adding the potential associated with repulsion of the fixed nuclei to the electronic energy.

For the majority of the calculations presented here, the set of basis functions chosen corresponds to a minimum basis set of Slater-type orbitals (STOs) centred at the respective nuclei:

$$\phi_u(\zeta,\underline{r}) = (\zeta^3/\pi)^{\frac{1}{2}} \exp(-\zeta r) \qquad \text{for 1s orbitals} \qquad \text{I-11}$$

$$\phi_u(\zeta,\underline{r}) = (\zeta^5/96\pi)^{\frac{1}{2}}\, r \exp(-\zeta r/2) \qquad \text{for 2s orbitals} \qquad \text{I-12}$$

$$\phi_u(\zeta,\underline{r}) = (\zeta^5/32\pi)^{\frac{1}{2}}\, r \exp(-\zeta r/3) \cos\theta \qquad \text{for } 2p_z \text{ orbitals} \qquad \text{I-13}$$

Here r is the distance from the nucleus on which the orbital is centred and ζ is the STO exponent. Expressions for the $2p_x$ and $2p_y$ orbitals are similar to I-13. This basis set has the advantage of being conceptually close to traditional chemical ideas of electronic structure and is generally considered to be the most appropriate for molecular orbital calculations. Because of the exponential form of the STOs however, the computation of the multicentre integrals $\langle uv|rs\rangle$ needed for the calculation of F_{uv} can be accomplished only by numerical quadrature, a difficult and time-consuming task. For this reason each STO is here represented by a linear combination of Gaussian functions. The corresponding integrals over these latter functions can be evaluated in closed form using the expressions originally derived by Boys (9).

The particular Gaussian representations used in this work are the STO-NG expansions developed by Pople and co-workers (10,11):

$$\phi_u(\zeta,\underline{r}) = \zeta^{\frac{3}{2}} \sum_n d_{un}\, g_u(\alpha_{un},\zeta\underline{r}) \qquad \text{I-14}$$

where $g_u(\alpha,\underline{r}) = (2\alpha/\pi)^{\frac{3}{4}} \exp(-\alpha r^2)$ for s orbitals I-15

$$g_u(\alpha,\underline{r}) = (128\alpha^5/\pi^3)^{\frac{1}{4}}\, r \exp(-\alpha r^2)\cos\theta \quad \text{for } p_z \text{ orbitals} \qquad \text{I-16}$$

In these expansions, the coefficients d_{un} and Gaussian exponents α_{un} are chosen to give a least-squares fit of the Gaussian representation to the STO. The STO exponents, ζ, are retained as variational parameters. A standard set of exponents (listed in Table I-1) has however been proposed (10,11) and, unless indicated otherwise, these exponents are used in the present calculations. All of the integrals over Gaussian functions have been evaluated using subroutines from the POLYATOM (12) and IBMOL (13) programs.

Although expansions are available for N=2 up to N=6, extensive studies by Pople and co-workers (10,14-17) have shown that the STO-3G expansion is the most economical to use for the accurate prediction of molecular geometries. The average deviations from experimental bond lengths and bond angles have been found to be 0.035 Å and 1.7° respectively for a large selection of first-row polyatomic molecules using such a basis set expansion. Many

TABLE I-1

Standard STO Exponents

Atom	Exponent		
	K Shell	L Shell	M Shell
H	1.24		
He	1.69		
Be	3.68	1.15	
B	4.65	1.50	
C	5.67	1.72	
N	6.67	1.95	
O	7.66	2.25	
F	8.65	2.55	
P	14.50	5.37	1.90
S	15.47	5.79	2.05

experimental trends (such as the progressive shortening of the C=C bond along the series propene-allene-cyclopropene (16)) are well reproduced. In addition, calculated dipole moments are in reasonable agreement with experimental values and charge distributions agree qualitatively with expectations from chemical reactivity (18).

For the accurate prediction of isomerization energies or enthalpies of reactions, however, the STO-3G basis set has been found to be unsatisfactory (15,16,19). For calculation of these properties, Pople and co-workers have proposed an extended basis set (20) containing more than the minimal number of ϕ_u functions. For this basis set, termed 4-31G, the inner-shell orbitals of heavy atoms are represented by a fixed linear combination of four Gaussian functions. The valence-shell orbitals (ie. hydrogen 1s and heavy atom 2s and 2p) are described by inner and outer parts which are respectively, sums of three and one Gaussian functions. The Gaussian functions have the same form as those in equation I-14, but for this basis set the coefficients d_{un} and exponents α_{un} have been determined by minimizing the calculated energy of the atomic ground states. The ζ exponents for the inner and outer parts of the valence shell orbitals are used as molecular scale factors to allow for changes in orbital size in a molecular environment. Standard values were determined by Pople and co-workers (20) by minimizing the ground state energy of a selected set of small polyatomic molecules. Although

predicted geometries are only marginally improved with the 4-31G basis set (15,17), total energies are predicted to be somewhat lower and the greater flexibility afforded by the "split" valence shell leads to greater reliability in the calculation of potential surfaces and to a large improvement in calculated relative energies of isomers. Because of the higher cost, however, the use of this basis set in the present calculations is restricted to those instances when the STO-3G results are expected to be unreliable.

Charge distributions and orbital populations for the molecules considered in Chapter III have been computed using the scheme proposed by Mulliken (21). In this method the total electron density is divided into two parts; that associated solely with single atomic orbitals ("net orbital populations") and that shared between pairs of orbitals ("overlap populations"). The electron density assigned to an atom in a molecule ("gross atomic population") is taken to be the sum of the net orbital populations for all the orbitals of that atom plus exactly one-half the overlap population between the orbitals of the atom in question and all the other orbitals in the molecule.

It is widely appreciated that the single determinant method discussed above does not make any provision for the correlation of the motion of electrons with antiparallel spin. The conventional way of compensating for this deficiency is to reformulate the molecular wave-

function and to express it as a linear combination of determinants Ψ_k, each of which is formed from the lowest energy configuration Ψ_0, by excitation of one or more electrons:

$$\Psi' = \Psi_0 + \sum_k c_k \Psi_k \qquad \text{I-17}$$

In principle a configuration interaction (CI) formulation can lead to an exact solution, but only in the unattainable limit of a complete set of configurations. In the calculations presented here, the gross errors of neglect of electron correlation are taken into account by carrying out a limited CI calculation using the most important configurations. Since the single determinant orbitals are determined self-consistently, Brillouin's Theorem (22) is assumed to apply at least approximately and thus configurations differing from the ground configuration by only one spin orbital can be neglected in the CI procedure since they do not interact directly with the lowest energy configuration. Further discussion of the configurations used is made in the context of the applications in Chapter III.

CHAPTER II

A COMPARISON OF THREE DIFFERENT METHODS FOR OBTAINING THE ENERGIES AND GEOMETRIES OF OPEN-SHELL SYSTEMS

(a) Introduction

It is well known that the calculation of wavefunctions and energies for molecules with unpaired electrons is considerably more complex than are the corresponding calculations for closed-shell systems. A number of methods have been proposed for dealing with the problem (8,23-26), the most widely used of which are the Roothaan restricted open-shell method (8) and the "unrestricted" method proposed by Pople and Nesbet (23). The former method however, besides being computationally expensive, is often plagued with convergence difficulties (27), while the latter suffers from the objection that the resultant wavefunction is not an eigenfunction of the operator $\hat{S}^2$. It therefore seems desirable to explore alternative methods for computing open-shell wavefunctions and energies. In particular, the contents of this chapter are concerned with the comparison of the energies of open-shell systems as calculated at three levels of sophistication - the Roothaan open-shell method, the "half-electron" method (28-30, see also ref. 31) and, in the case of triplets, the simple use of optimum ground state eigenvectors for the excited state.

The half-electron method was developed primarily for use in semiempirical calculations (28,29) and contains one fundamental approximation; namely that each unpaired elec-

tron is replaced by two "half-electrons" of opposite spin and a calculation employing the usual closed-shell methods is carried out on the resulting pseudo-closed-shell system. Thus the method retains the computational simplicity and speed of a closed-shell, single determinant calculation, while employing the correct populations for the molecular orbitals in the open-shell problem. An "error" occurs because the quantity which is minimized in determining the MO coefficients does not correspond exactly to the energy of a radical or a triplet state. Specifically, a spurious Coulomb repulsion between the two half-electrons in the singly-occupied orbitals is always included. In addition, for triplet states the exchange repulsion term between the electrons in the two open-shell orbitals is underestimated by one-half. The method does account properly for the total one-electron energy and for the two-electron terms arising from the Coulomb and exchange repulsion of the electrons in doubly-occupied orbitals with one another and with the electron(s) in the singly-occupied orbital(s), and from the Coulomb repulsion of the unpaired electrons in different orbitals. Thus the quality of the half-electron method wavefunction is affected by the extent to which the wavefunction is altered by minimizing not the true energy but the true energy plus the errors mentioned above.

The second alternative method considered here, i.e. the use of the eigenvectors from the closed-shell ground state to represent the triplet wavefunction, has been widely used

in both semiempirical and ab initio calculations for excited states. The errors in this approach can be expected to be somewhat larger than for the half-electron method however, since the determination of the MO coefficients is carried out with the ground state (closed-shell) Fock operator, without regard for the populations of the MOs in the triplet state. Thus the difference between the energy determined by this method and the true open-shell energy is a reflection of the extent of orbital reorganization which accompanies the excitation from closed to open shell.

The intention here is to make a thorough and quantitative comparison between the three techniques mentioned above in the context of ab initio calculations of the total energy and of the predicted geometries for polyatomic radicals and triplets. To this end, the half-electron and Roothaan open-shell procedures are compared on a formal basis in the next section, and the performance of the three methods is compared for eight different radicals and nineteen different triplets in the third section.

(b) Theory

The expectation value for the energy of an open-shell configuration is given in Roothaan's formulation(8), by equation II-1, in which f, a, and b are numerical constants:[1]

---

[1]Following Roothaan, the indices k and l are used for the individual closed-shell orbitals, m and n for the open-

$$E = 2\sum_k I_k + \sum_k\sum_l (2J_{kl} - K_{kl}) + f\{2\sum_m I_m + f\sum_m\sum_n (2aJ_{mn} - bK_{mn}) + 2\sum_k\sum_m (2J_{km} - K_{km})\} \quad \text{II-1}$$

Most radicals and triplets can be classified as "half-filled" shells (i.e. the same number of open-shell electrons as occupied open-shell orbitals, with all spins parallel in singly-occupied orbitals) in which case f,a and b take on the fixed values of ½, 1 and 2 respectively (8). Equation II-1 then simplifies to the form:

$$E = 2\sum_k I_k + \sum_k\sum_l (2J_{kl} - K_{kl}) + \sum_m I_m + \tfrac{1}{2}\sum_m\sum_n (J_{mn} - K_{mn}) + \sum_k\sum_m (2J_{km} - K_{km}) \quad \text{II-2}$$

In the half-electron method, the quantity E', minimized in the SCF process is given by a modification of the usual closed-shell expression (28):

$$E' = \sum_i N_i I_i + \tfrac{1}{2}\sum_i\sum_j N_i N_j (2J_{ij} - K_{ij}) \quad \text{II-3}$$

Here N_i and N_j represent the occupation numbers (0, 1, or 2 electrons) of molecular orbitals i and j. Expansion of II-3 for the half-filled shell leads to

$$E' = 2\sum_k I_k + \sum_m I_m + \sum_k\sum_l (2J_{kl} - K_{kl}) + \tfrac{1}{2}\sum_m\sum_n (2J_{mn} - K_{mn}) + \sum_k\sum_m (2J_{km} - K_{km}) \quad \text{II-4}$$

---

shell orbitals and i and j for the orbitals of either set. The integrals used in II-1 are defined as:

$I_i = \langle \psi_i^*(1) | T+V | \psi_i^*(1) \rangle$

$J_{ij} = \langle \psi_i^*(1)\psi_j^*(2) | 1/r_{12} | \psi_i(1)\psi_j(2) \rangle$

$K_{ij} = \langle \psi_i^*(1)\psi_j^*(2) | 1/r_{12} | \psi_i(2)\psi_j(1) \rangle$

The only difference between the true energy E of equation II-2 and the quantity E' of equation II-4 is the term associated with the singly-occupied orbitals:

$$E - E' = \tfrac{1}{2}\sum_m \sum_n (J_{mn} - K_{mn}) - \tfrac{1}{4}\sum_m \sum_n (2J_{mn} - K_{mn})$$
$$= -\tfrac{1}{4}\sum_m \sum_n K_{mn} \qquad \text{II-5}$$

This is the correction which must be applied to E' after convergence of the SCF process to yield the half-electron approximation to the open-shell energy.

An appreciation of the effect of this spurious term on the wavefunctions determined by the half-electron method can be gained by examining the diatomic radical HeH. In the LCAO-MO formulation, the MOs can be written as

$$\psi_1 = c_{11}\phi_H + c_{12}\phi_{He}$$
$$\psi_2 = c_{21}\phi_H + c_{22}\phi_{He} \qquad \text{II-6}$$

Here ψ_1 is the doubly-occupied, bonding MO and ψ_2 is the singly-occupied, antibonding MO. Given any arbitrary value for one of the four coefficients (say c_{11}) and a value for the overlap integral $S_{1'2}$, the other three coefficients can be determined easily using orthogonality and normalization conditions. Thus, both the Roothaan energy E and the quantity E' can be calculated as a function of c_{11}; the results are plotted against c_{11} for the range of interest in Figure II-1.[2] The minimum for the E function

---

[2]These results refer to calculations which were

FIGURE II-1

The Roothaan Energy, E and the Quantity, E' versus c_{11} for HeH.

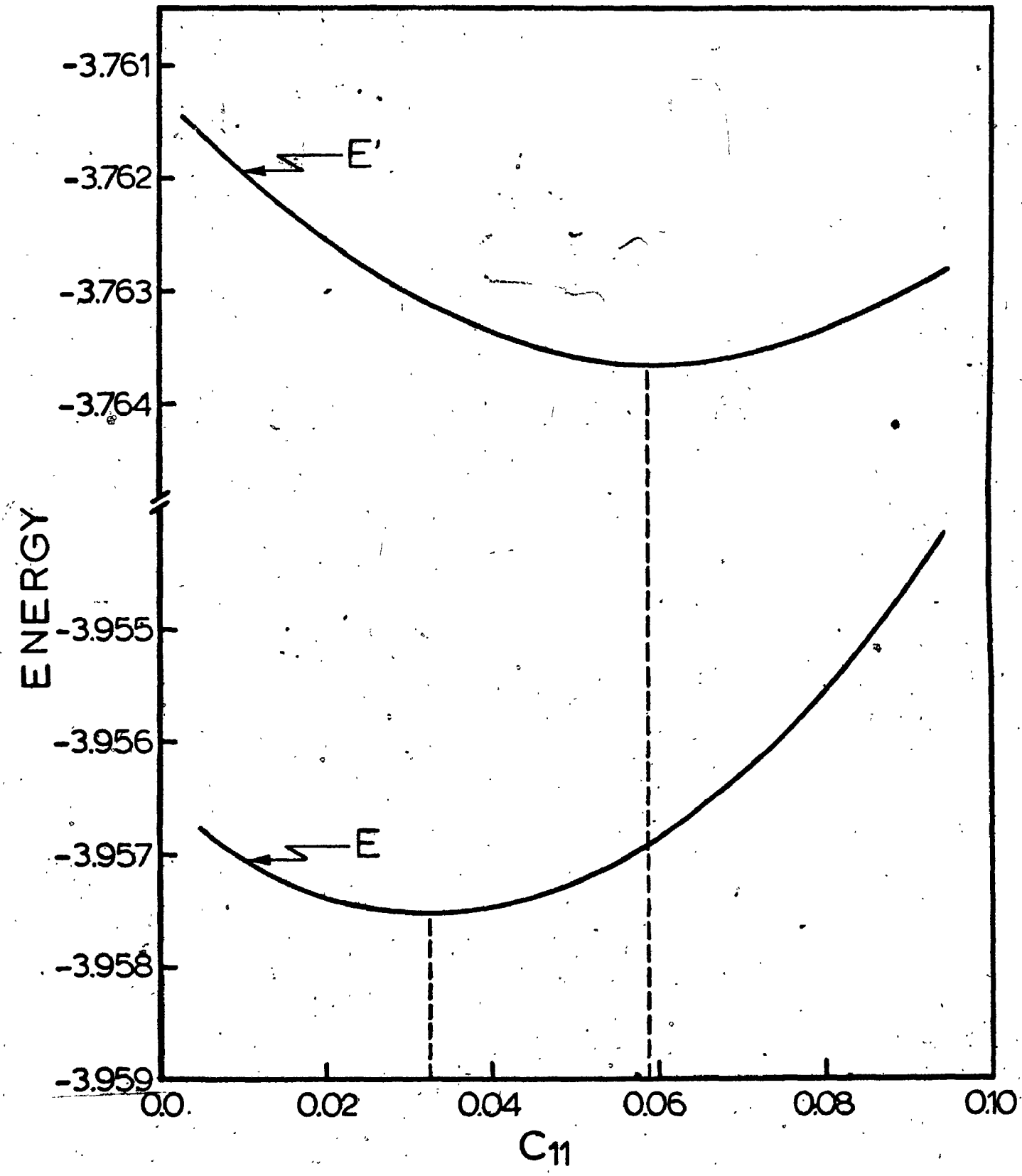
-3.761
-3.762
-3.763
-3.764
E'
E
-3.955
-3.956
-3.957
-3.958
-3.959
ENERGY
0.0
0.02
0.04
0.06
0.08
0.10
C11

occurs at $c_{11} = 0.033$ whereas that for E' occurs at $c_{11} = 0.059$; complete wavefunctions for these points are listed in Table II-1. The extra delocalization of the electron density in the singly-occupied orbital in the half-electron wavefunction as compared to that in the Roothaan wavefunction is consistent with the attempt of the former method to minimize the repulsion of the two half-electrons. In general, this effect will always be present for a radical since from equation II-5:

$$E' = E + K_{22}/4 = E + J_{22}/4 \qquad \text{II-7}$$

Although the difference in energy between the two methods amounts to only 0.0006 a.u. for HeH, the difference is gnerally expected to be larger for triplet states since E' then contains three, rather than just one spurious terms:

$$E' = E + J_{mm}/4 + J_{nn}/4 + K_{mn}/2 \qquad \text{II-8}$$

Carsky and Zahradnik have discussed several instances from semiempirical calculations in which the Roothaan and half-electron methods yield identical energies and wavefunctions (32). This will always occur in minimal basis set calculations in which the singly-occupied MOs are completely determined by symmetry, since the spurious terms in E' involve only the singly-occupied MOs and are constants

---

carried out using the STO-4G basis set with standard exponents and an He-H separation of 1.5875 Å.

TABLE II-1

SCF Wavefunctions For HeH

(a) Calculated With Roothaan's Method

MO	AO	
	ϕ_H	ϕ_{He}
ψ_1	0.0328	0.9946
ψ_2	1.0108	-0.1832

electronic energy = -3.95752 a.u.

(b) Calculated With the Half-Electron Method

MO	AO	
	ϕ_H	ϕ_{He}
ψ_1	0.0593	0.9894
ψ_2	1.0096	-0.2093

electronic energy = -3.95690 a.u.

in such cases. In general, the Fock operators for the open and closed shells in the Roothaan method differ from the Fock operator for the half-electron method:

$$\hat{F}_c = \hat{F}_{\frac{1}{2}} + \sum_m \hat{M}_m \qquad \text{for doubly-occupied MOs k} \qquad \text{II-9}$$

$$\hat{F}_o = \hat{F}_{\frac{1}{2}} + \sum_k \hat{M}_k - \tfrac{1}{2}\sum_m \hat{K}_m \qquad \text{for singly-occupied MOs m} \qquad \text{II-10}$$

Here $\hat{K}_m$ is the familiar exchange operator and $\hat{M}_k$ and $\hat{M}_m$ are exchange coupling operators, defined in general by equation II-11:

$$\hat{M}_i = \langle\psi_i|\hat{K}_o|\psi\rangle\psi_i + \langle\psi_i|\psi\rangle\hat{K}_o\psi_i \qquad \text{II-11}$$

$$\text{where } \hat{K}_o = \tfrac{1}{2}\sum_m \hat{K}_m$$

The effect of the closed-shell Fock operator, $\hat{F}_c$ and that of the half-electron Fock operator on an arbitrary function from the closed-shell set is the same, however:

$$\hat{F}_c\psi_k = \hat{F}_{\frac{1}{2}}\psi_k \qquad \text{II-12}$$

Thus the eigenvalues, η_k of the closed-shell operator, $\hat{F}_c$ are identical with the eigenvalues of $\hat{F}_{\frac{1}{2}}$:

$$\hat{F}_c\psi_k = \eta_k\psi_k \qquad \text{II-13}$$

$$\hat{F}_{\frac{1}{2}}\psi_k = \eta_k\psi_k \qquad \text{II-14}$$

Note that the eigenvectors of $\hat{F}_c$ must be identical to those deduced from $\hat{F}_{\frac{1}{2}}$ whenever the singly-occupied orbitals are symmetry determined. For the singly-occupied orbitals,

even in symmetry-determined cases, the eigenvalues of $\hat{F}_o$ and $\hat{F}_{\frac{1}{2}}$ differ:

$$\hat{F}_o\psi_m = \eta_m\psi_m \qquad \text{II-15}$$

$$\text{but} \quad \hat{F}_{\frac{1}{2}}\psi_m = \varepsilon_m\psi_m \qquad \text{II-16}$$

If the Roothaan method is formulated in terms of a single Fock operator, $\hat{F}$, however, the eigenvalues of the singly-occupied orbitals in the two methods become identical, but those of the doubly-occupied MOs differ:

$$\hat{F}\psi_k = \varepsilon_k\psi_k \qquad \text{II-17}$$

$$= (\eta_k + \zeta_k)\psi_k \qquad \text{II-18}$$

$$\text{where } \zeta_k = \sum_m K_{km} \qquad \text{II-19}$$

$$\hat{F}\psi_m = \varepsilon_m\psi_m \qquad \text{II-20}$$

Thus, for symmetry-determined cases, the eigenvalues for the closed-shell orbitals as determined by the two methods differ by the exchange integrals K_{km} while the eigenvalues for the open-shell orbitals are identical. Since the eigenvectors for both sets of orbitals are identical, the total energies determined by the Roothaan and half-electron methods will also be identical. These arguments are more generally applicable than those given by Carsky and Zahradnik who arrive at this latter conclusion only for special cases in which the exchange integrals, K_{km} of equation II-19 are zero. The conclusions presented here have

also been tested by calculations on several symmetry-determined systems, namely, planar CH_3, NH_2, planar $C_2H_4^+$, planar $C_2H_4^-$ and the planar $^3(\pi,\pi^*)$ state of C_2H_4; in all cases the total energy deduced by the Roothaan scheme and the half-electron method agreed exactly, whereas the doubly-occupied MO eigenvalues of $\hat{F}$ and $\hat{F}_{\frac{1}{2}}$ differed since the exchange integrals, K_{km}, were nonzero.

(c) Results and Discussion

In order to compare quantitatively the performance of the three methods, ab initio calculations using the STO-3G expansions have been performed for a number of radicals and triplets.

The total energies for the ground states of eight small free radicals calculated by the Roothaan open-shell method are compared in Table II-2 with those calculated for the same geometries by the half-electron procedure. (Calculations for CH_3, NH_2, $C_2H_4^+$ and $C_2H_4^-$ have been omitted since the singly-occupied MOs are determined by symmetry in the STO-3G approximation, with the result that the energies calculated by the two methods are identical.) The root mean square improvement in the energy using the Roothaan wavefunctions is 0.0076 a.u., or 4.8 kcal mol^{-1}. Given this difference, it might be expected that the geometries predicted by the two methods for such radicals would differ significantly. However, complete optimization of the geometrical structures of HCO, NO_2 and NF_2 pro-

TABLE II-2

Energies (in a.u.) for Ground States of Free Radicals

Radical	State Designation	Roothaan Energy	Roothaan Method Energy Improvement over Half-Electron Method
BH_2[a]	$^2A_1$	-25.40817	0.00234
H_2CN[b]	$^2B_2$	-92.23328	0.00985
H_2NO[c]	$^2B_1$	-128.67874	0.01447
HCO[a]	$^2A'$	-111.72751	0.00129
C_2H_3[d]	$^2A'$	-76.41135	0.00796
C_2H_5[d]	$^2A'$	-77.65919	0.00458
NO_2[a]	$^2A_1$	-201.26761	0.00060
NF_2[a]	$^2B_1$	-249.74005	0.00810

[a]Calculated using experimental geometry given in reference 33.

[b]Geometry assumed (34): R(CN)=1.273Å, R(CH)=1.88Å, angle (HCN)=121.5°.

[c]Calculated using geometry given in reference 35.

[d]Calculated using geometry given in reference 15.

duce r.m.s. differences of only ±0.003 Å in the bond lengths and ±0.5° in the bond angles (see Table II-3). Thus the energetic inferiority of the half-electron wavefunction is appreciable but is almost independent of geometry for these radicals.

As anticipated earlier, the errors associated with the half-electron method are greater for triplet states than for free radicals. For the nineteen molecules listed in Table II-4, the r.m.s. energy improvement using the Roothaan open-shell wavefunction relative to that of the half-electron procedure is 0.013 a.u., or 8.2 kcal mol^{-1}. In addition, the differences in optimum geometrical structures for the six triplet states documented in Table II-5 are also somewhat larger than for the free radicals; the r.m.s. deviation in the bond distances is ±0.007 Å and in the bond angles ±2.4°.

For fifteen of the nineteen triplets listed in Table II-4, the half-electron method yields an energy superior to that obtained using MOs of the lowest closed-shell singlet state. On the average the energy obtained using the closed-shell eigenvectors is much farther from the Roothaan open-shell result (r.m.s. deviation of 0.042 a.u., or 26 kcal mol^{-1}) than is the half-electron energy (r.m.s. deviation of 0.013 a.u., or 8.2 kcal mol^{-1}). In addition, the magnitude of the energy improvement from the closed-shell result is much less predictable than is that from the half-electron results, since the standard

TABLE II-3

Predicted and Experimental Geometries of HCO, NO_2 and NF_2

Radical	State	Parameter[a]	Method		Experimental[b]
			Half-electron	Roothaan	
HCO	$^2A'$	R(CO)	1.19_5	1.19_4	1.198
		R(CH)	1.11_1	1.11_4	1.08
		angle (CHO)	125.8	126.6	119.5
		total energy	-111.72665	-111.72927	
NO_2	$^2A_1$	R(NO)	1.23_6	1.23_6	1.1934
		angle (ONO)	134.2	134.6	134.1
		total energy	-201.27620	-201.27679	
NF_2	$^2B_1$	R(NF)	1.35_5	1.36_1	1.37
		angle (FNF)	101.9	101.9	104.2
		total energy	-249.7326	-249.7404	

[a]Bond lengths are in Å, angles in degrees, and energies in a.u.

[b]Experimental geometries from reference 33.

TABLE II-4

Calculated Energies (in a.u.) for Triplet States

Molecule[a]	State Designation	Roothaan Energy	Roothaan Method Energy Improvement over Half-Electron Method	Roothaan Method Energy Improvement over Closed-Shell Orbitals
CH_2(36)	$^3B_1$	-38.42916	0.00617	0.00316
NH_2^+(17)	$^3B_1$	-54.54242	0.00418	0.00122
C_2H_2(37)	$^3B_2$	-75.74540	0.01074	0.01523
C_2H_4(38)	$^3A_2$	-77.01162	0.00855	0.00887
C_4H_6(39)	^3B_u	-152.90442	0.01533	0.03195
HCF(33)	$^3A''$	-135.89433	0.01168	0.01125
CF_2(40)	$^3B_1$	-233.36019	0.01190	0.01409
CH_3CH(36,41)	$^3A''$	-77.01453	0.01523	0.02156
HCN(33)	$^3A''$	-91.54580	0.01587	0.02753
HCP(33)	$^3A''$	-374.68753	0.00731	0.00676
HNO(33)	$^3A''$	-126.07196	0.01331	0.01827
HNNH(42)	^3B	-108.51529	0.01732	0.02250
H_2BNH_2(34)	$^3A_2$	-80.28197	0.02033	0.05941
H_2CNH(43)	$^3A''$	-92.77203	0.01147	0.10944
H_2NN(44)	$^3A''$	-108.58886	0.01711	0.01907
H_2CO(33)	$^3A''$	-112.31850	0.01824	0.07535
H_2CS(45)	$^3A_2$	-431.65805	0.01117	0.06080
NCN(33)	$^3\Sigma_g^-$	-144.75811	0.00000	0.02061
O_3(46)	$^3B_2$	-221.42485	0.01640	0.06035

[a]The numbers in parentheses refer to the reference from which the molecular geometry was taken. In some cases the geometry of the triplet state is not known experimentally and is estimated from the geometry of the singlet state of the same electron configuration.

deviation from the mean deviation of the former is five times that of the latter.

It is instructive to consider more closely the five triplets in Table VI-4 for which the use of closed-shell eigenvectors leads to an energy which is especially poor in relation to that obtained with the open-shell methods. In particular, for the triplets of H_2CO, H_2CS, H_2CNH, O_3 and H_2BNH_2, the energy improvement using the Roothaan method is greater than 0.05 a.u.. In all five cases, the electronic charge distribution in the triplet state is significantly different from that in the ground state since the excitation involves moving an electron from a highly localized non-bonding orbital to an antibonding orbital localized in another region of space. Evidently, the charge reorganization accompanying such an excitation is handled rather well by the half-electron method, since the half-electron to Roothaan energy improvement for these five cases averages one-quarter the closed-shell to Roothaan energy difference. This conclusion is illustrated particularly well by an analysis of the MO coefficients predicted by the three methods for formaldehyde. The $^3(n\pi^*)$ state of H_2CO is formed by the excitation of an electron from the non-bonding b_2 orbital in the plane of the molecule and localized on the oxygen atom to the antibonding π^* orbital above and below the molecular plane. In the ground state, the π and π^* orbitals are polarized slightly toward the oxygen and

carbon atoms respectively. Use of these orbitals to describe the triplet state leads to an excited state charge distribution in which the carbon atom carries a substantial negative charge and the oxygen atom a substantial positive charge (see Table II-5). In contrast, both open-shell methods predict a significant reorganization of the π and π^* orbitals so that the former is localized primarily on oxygen and the latter on carbon. This results in the prediction of slight net negative charges for both oxygen and carbon as shown in Table II-5 for the lowest triplet state.

The reorganization of the electron distribution in the half-electron and Roothaan methods also leads to an optimum geometry for the $^3(n\pi^*)$ state of H_2CO which is significantly different from that predicted using closed-shell eigenvectors. In particular, the carbon-oxygen bond length elongation (compared to the ground state) is predicted to be $\simeq 0.2$Å according to the first two methods, compared to $\simeq 0.1$Å according to the latter (see Table II-6). In addition, use of the closed-shell wavefunctions yields a planar, rather than a pyramidal "flapped" geometry, for the $^3(n\pi^*)$ state. For the other triplets listed in Table II-6, the excitation does not involve as much charge transfer and the agreement between the closed-shell and open-shell wavefunction geometries is rather good.

TABLE II-5

Gross Orbital and Atomic Populations Predicted for the $^3(n\pi^*)$ State of H_2CO

Atom	Orbital[a]	Gross Population (in e)		
		Roothaan Method	Half-Electron Method	Closed-Shell Orbitals
H	1s	0.9304	0.9158	0.8573
C	1s	1.9933	1.9932	1.9937
	2s	1.1805	1.1883	1.2381
	$2p_x$	1.1072	1.1632	1.3891
	$2p_y$	1.0016	0.9706	0.9611
	$2p_z$	0.7715	0.7733	0.8581
total atomic		6.0541	6.0886	6.4401
O	1s	1.9985	1.9985	1.9985
	2s	1.9021	1.9001	1.8935
	$2p_x$	1.8319	1.7607	1.5076
	$2p_y$	1.0106	1.0690	1.1686
	$2p_z$	1.3419	1.3514	1.2766
total atomic		8.0850	8.0797	7.8448

[a] The coordinate system was chosen with the origin at the carbon atom, the positive z axis coincident with the C-O bond, the y axis in the HCH plane and the x axis mutually perpendicular to y and z. The experimental geometry was taken from reference 33.

TABLE II-6

Predicted Geometries for Six Triplet States

Molecule	State	Parameter[a]	Method		
			Roothaan	Half-Electron	Closed-Shell Orbitals
CH_2	$^3B_1$	R(CH)	1.082	1.078	1.079
		angle (HCH)	124.	125.	124.
		total energy	-38.43174	-38.42504	-38.42860
CO	$^3\Pi$	R(CO)	1.220	1.222	1.227
		total energy	-111.03651	-111.02353	-111.02524
NCN	$^3\Sigma g^-$	R(CN)	1.238	1.239	1.231
		angle (NCN)	180.	180.	180.
		total energy	-144.75825	-144.75830	-144.73750
H_2CO	$^3A''$	R(CO)	1.395	1.411	1.318
	$^3(n\pi^*)$	R(CH)	1.088	1.077	1.062
		angle (HCH)	117.	121.	125.
		β[b]	37.	36.	0,0
		total energy	-112.32588	-112.31043	-112.24651
H_2CO	$^3A'$	R(CO)	1.472	1.470	1.456
	$^3(\pi\pi^*)$	R(CH)	1.092	1.087	1.081
		angle (HCH)	115.5	118.8	121.6
		β[b]	36.	23.	23.
		total energy	-112.29489	-112.29118	-112.28875
C_2H_2	$^3B_2$	R(CO)	1.314	1.313	1.316
		R(CH)	1.091	1.085	1.084
		angle (HCC)	126. (cis)	127. (cis)	126. (cis)
		total energy	-75.74567	-75.73479	-75.73046

[a] Bond lengths are in Å, angles in degrees, energies in a.u..

[b] β is the angle between the HCH plane and CO bond.

(d) Conclusions

The half-electron method, although not converging to the wavefunction yielding the lowest total energy because of the inclusion of spurious correction terms, is generally superior to the use of eigenvectors deduced for the lowest closed-shell singlet state. This effect is particularly noticeable when the electronic charge distribution in the triplet state differs appreciably from that in the ground state. The r.m.s. deviations between the half-electron and the Roothaan open-shell energies of ≈5 and ≈8 kcal mol^{-1} for radicals and triplet states, respectively are probably too great for the former method to be used instead of the latter in applications where total energies, rather than geometries, are of prime importance. In practice, the half-electron method is significantly faster, computationally than is the Roothaan method and in many cases the use of the half-electron wavefunction as an "initial guess" for the Roothaan procedure decreases the number of iterations (and thus the computational expense) required to reach an SCF solution. In addition, this technique can often overcome the tendency of the Roothaan method to either diverge, or converge to a higher excited state.

CHAPTER III

APPLICATIONS TO CHEMICAL SYSTEMS

1. The Bonding, Structure and Energetics in Alkyl and Aminoberyllium Compounds

(a) Introduction

Compared to that of the other group II elements of the periodic table, the organic chemistry of beryllium has been relatively neglected. The extreme toxicity of organoberyllium compounds and their tendency to aggregate (or, in solution, to coordinate with the solvent) has often made it difficult to carry out the usual experiments in structure determination. Several reviews (47,48,49) have appeared on the subject and, although these indicate that some progress has been made in the synthesis of these species, they also indicate a lack of quantitative physical data pertaining to bonding and energetics.

The available information relates primarily to the dialkyl derivatives and indicates that organoberyllium compounds, like their magnesium counterparts, have covalent bonds of a highly polar nature and, like the boranes, exhibit "electron-deficient" bonding. For this reason, semiempirical molecular orbital methods are particularly unsuited to the calculation of wavefunctions for these systems and their use has led to some rather unrealistic results. For example, calculations of the Extended Huckel type (50) predict that the beryllium and carbon atoms in

the dimethylberyllium monomer carry charges of +1.83 and -1.18e respectively. In addition, these calculations predict that the dimethylberyllium dimer is more than 180 kcal mol^{-1} more stable than two monomers. Given that, in the gas, dimethylberyllium is found to be predominantly monomeric (51), this latter prediction cannot be taken seriously.

The ab initio calculations presented here, the first to be carried out for organoberyllium compounds, were undertaken in order to deduce the bonding (e.g., the ionic versus covalent character, the degree of hyperconjugation, etc.) in both alkyl and aminoberyllium derivatives, the optimum geometries for $HBeCH_3$ and $HBeNH_2$ monomers, and the nature of the monomer-monomer interactions.

(b) Alkylberyllium Compounds

In contrast to the lithium alkyls which are found in tetrameric or hexameric form (52,53), beryllium alkyls are usually found in lower degrees of association. Dimethylberyllium, for instance, is found to be polymeric in the solid (54), but monomeric (51) in the gas phase. The diethyl, di-n-propyl, diisopropyl, di-n-butyl and diisobutyl derivatives are all found to be dimeric in benzene (55) while di-t-butylberyllium is found in monomeric form only. For this latter compound, dimerization is thought to be prevented by the steric interactions of the voluminous t-butyl groups (49). For the dimethyl derivative, however, the unusual stability of the

monomer has been attributed to a hyperconjugative effect (51) as represented by the valence bond structures (1a) and (1b). Support for this mechanism is based on the ob-

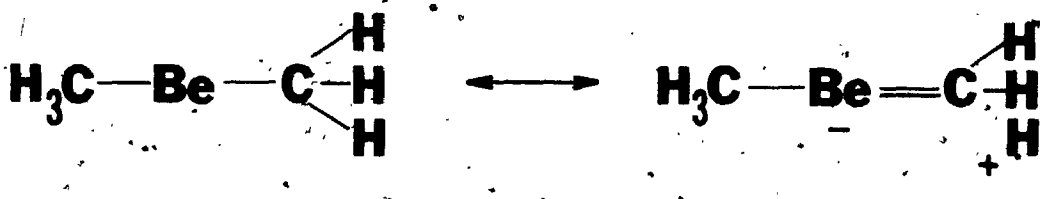

(1a) (1b)

servation that the C-Be-C asymmetric stretching frequency of 1081 cm^{-1} in dimethylberyllium is considerably higher than the value of 450 cm^{-1} measured for di-t-butylberyllium and on the assertion that hyperconjugation in the di-t-butyl derivative is negligible. However, Almenningen et al. (56) suggest that significant hyperconjugation should be manifested by a shortening of the Be-C bond distance in the dimethyl derivative relative to the di-t-butyl derivative and, since they do not observe this shortening effect, conclude that hyperconjugation is relatively unimportant. In addition, there is ample evidence from other sources (57) which indicates that there is little or no difference between the stablization afforded by methyl groups and that afforded by t-butyl groups. Nevertheless, the beryllium atom is geometrically well-disposed to receive electron density by this mechanism and the hyperconjugative stablization may amount to somewhat more than the usual 1-2 kcal mol^{-1} (57).

To deduce the strength of the quasi-π bond of (1b), STO-3G calculations were carried out on the hypothetical beryllium alkyl $HBeCH_3$ and on $Be(CH_3)_2$. Two basis sets were used; one with a full 1s, 2s, 2p set of orbitals on the beryllium atom and one with only 1s, 2s, and $2p_\sigma$ orbitals on beryllium. Removal of the beryllium $2p_\pi$ orbitals in the second basis set constrains the Be-C linkages to σ-bonding only. The energy difference between calculations with the two basis sets then represents the stabilization afforded by the "back-release" of electrons from carbon to beryllium. First a partial exponent optimization was carried out on $HBeCH_3$ to introduce some anisotropy into the basis sets (see Table III-1 for the resultant exponents and details of the procedure). Then, with the full basis set on beryllium, and assuming C-H distances of 1.094 Å and exactly tetrahedral HCH angles, the Be-C and H-Be bond lengths in $HBeCH_3$ were optimized and found to be 1.71 and 1.33 Å respectively. (The former agrees well with the electron diffraction values of 1.698 and 1.699 Å for dimethylberyllium (56) and di-t-butylberyllium (59), respectively). The total energy for $HBeCH_3$ in this geometry with the full basis set is calculated to be -54.16140 a.u. compared to an energy of -54.15004 a.u. calculated with the partial basis set. Thus, the energy gain by allowing hyperconjugation to operate is calculated to be 7.1 kcal mol^{-1} for one methyl group.

A similar STO-3G calculation on $Be(CH_3)_2$ was carried

TABLE III-1

STO Exponents Found for $HBeCH_3$ and $HBeNH_2$[a]

Molecule	Atom	Orbital	Exponent
$HBeCH_3$	Be	1s	3.6848
		$2s,2p_\sigma$	1.12
		$2p_\pi$	0.75
	C	1s	5.6727
		2s,2p	1.68
	H(C)	1s	1.24
	H(Be)	1s	1.12
$HBeNH_2$	Be	1s	3.6848
		$2s,2p_\sigma$	1.12
		$2p_\pi$	0.82
	N	1s	6.6651
		$2s,2p_\sigma,2p_\sigma$	1.92
		$2p_\pi$	1.79
	H(N)	1s	1.24
	H(Be)	1s	1.12

[a]Exponent for the 1s orbital of the H atom bonded Be is the value which is optimum for BeH_2; while for the methyl and amino hydrogens the standard values are used. Exponents for the 1s orbitals of the heavier atoms are those established to be optimum for the free atoms (58). Valence shell σ orbital exponents for these atoms in $HBeCH_3$ are the result of an optimization using the 1s, 2s, $2p_\sigma$ basis set on beryllium. Exponents for the $2p_\pi$ orbitals are those found to be optimum for $HBeCH_3$ using these σ exponents. For $HBeNH_2$, the Be and N valence shell σ exponents are the result of an optimization with the $2p_\pi$ orbital included. Exponents for the π orbitals are optimum values using these σ exponents. In all cases, the starting value for the exponent variation was the standard value.

out using the beryllium and carbon exponents found for $HBeCH_3$ (Table III-1) and employing Be-C bond lengths of 1.71 Å. Tetrahedral HCH angles and C-H bond distances of 1.094 Å were assumed here also. A staggered conformation was assumed for the methyl hydrogens. The total energy of -92.74746 a.u. for the full basis set is 13.9 kcal mol^{-1} more negative than the value of -92.72535 a.u. determined with the partial basis set. Thus, the extent of π-bonding in this system is considerably greater than that usually attributed to hyperconjugation.

The SCF wavefunction, overlap population and both orbital and gross populations for $Be(CH_3)_2$ (using the full basis set) are given in Tables III-2, III-3 and III-4, respectively. For comparison, the overlap, orbital and gross populations for the partial basis set are also included. In both cases the calculated net atomic charges are more in line with chemical intuition than are those predicted by the Extended Huckel Method (50). The charges on the carbon atoms are essentially constant in the two basis sets, while the decrease in electron density on beryllium without the p_π orbitals is reflected in an increase in electron density on the methyl hydrogens. The cyclic pattern of σ-withdrawal/π-donation is also evident from the changes in carbon orbital populations on removal of the $2p_\pi$ orbitals of beryllium (i.e., an increase in electron density in the $2p_x$ and $2p_y$ orbitals with an accompanying decrease in the 2s and $2p_z$ orbitals).

TABLE III-2

SCF Wavefunction for $Be(H_2)_2$

Molecular Orbital	Atomic Orbitals																					Orbital Energy
	H_1	H_2	H_3	C_1					Be					C_2					H_4	H_5	H_6	
(D_{3d})	1s	1s	1s	1s	2s	$2p_x$	$2p_y$	$2p_z$	1s	2s	$2p_x$	$2p_y$	$2p_z$	1s	2s	$2p_x$	$2p_y$	$2p_z$	1s	1s	1s	(a.u.)
$1a_{2u}$	.0046	.0046	.0046	-.7014	-.0291			-.0010					-.0008	.7016	.0291			-.0010	-.0047	-.0047	-.0047	-11.0119
$1a_{1g}$	.0048	.0048	.0048	-.7018	-.0266			.0006	-.0003	.0026				-.7016	-.0266			-.0006	.0047	.0047	.0047	-11.0117
$2a_{1g}$	-.0019	-.0019	-.0019	-.0006	-.0019			.0002	.9913	.0323				-.0006	-.0019			-.0002	-.0019	-.0019	-.0019	-4.5080
$3a_{1g}$	.1363	.1363	.1363	-.1526	.4608			-.0289	-.0661	.0822				-.1526	.4608			.0289	.1364	.1363	.1363	-0.8755
$2a_{2u}$	.1367	.1367	.1367	-.1531	.4537			-.0374					-.0808	.1531	-.4537			-.0374	-.1367	-.1367	-.1367	-0.8724
$1e_u$	.3282	-.1652	-.1630			.0015	-.3853				.0004	-.1146				.0015	-.3853		-.3282	.1630	.1652	-0.5111
$1e_u$	-.0013	-.2836	.2848			.3853	.0015				.1146	.0004				.3853	.0015		.0013	-.2848	.2836	-0.5111
$1e_g$	.0011	-.3011	.3000			.4029	-.0013									-.4029	.0013		.0011	.3000	-.3011	-0.5005
$1e_g$	-.3471	.1726	.1745			.0013	.4029									-.0013	-.4029		-.3471	.1745	.1726	-0.5005
$4a_{1g}$	-.1093	-.1093	-.1093	-.0124	.0474			.4408	-.2094	.5342	-1.0606	-.0320		-.0124	.0474			-.4408	-.1093	-.1093	-.1093	-0.4087
$3a_{2u}$	.1150	.1150	.1150	.0248	-.0606			-.4734			.0320	-1.0606	.4576	-.0248	.0606			-.4734	-.1150	-.1150	-.1150	-0.3689
$2e_u$	-.0065	-.1835	.1900			.1473	.0044									.1473	.0044		.0065	-.1900	.1835	+0.1603
$2e_u$	-.2157	.1135	.1022			-.0044	.1473									-.0044	.1473		.2157	-.1022	-.1135	+0.1603

[a] The coordinate system is chosen with the beryllium atom at the origin, the positive z axis coincident with the Be-C_2 bond and hydrogen atoms H_1 and H_4 lying in the yz plane.

TABLE III-3

Atom-Atom Overlap Populations in $Be(CH_3)_2$

Atom Pair	Overlap Population (in e)	
	with p_π	without p_π
$Be-C_1(\sigma)$	0.6903	0.6921
$Be-C_1(\pi)$	0.0867	—
$Be-C_1$(total)	0.7770	0.6921
C_1-C_2	-0.0029	-0.0027
$C_1-H(C_1)$	0.7606	0.7862
$C_1-H(C_2)$	0.0001	0.0001
Be-H	-0.0412	-0.0699
$H(C_1)-H(C_1)$	-0.0346	-0.0372
$H(C_1)-H(C_2)$	0.0	0.0

TABLE III-4

Gross Populations for Orbitals and Atoms in $Be(CH_3)_2$

Atom	Orbital[a]	Gross Population (in e)	
		with p_π	without p_π
Be	1s	1.9934	1.9936
	2s	0.8070	0.8400
	$2p_\sigma$	0.6919	0.7182
	total σ	1.4989	1.5582
	$2p_x = 2p_y$	0.1055	—
	total π	0.2110	—
	total atomic	3.7033	3.5518
C	1s	1.9922	1.9922
	2s	1.2391	1.2315
	$2p_\sigma$	1.1950	1.1620
	$2p_x = 2p_y$	1.0014	1.0261
	total atomic	6.4291	6.4379
H	1s	0.9064	0.9288

[a] see footnote, Table III-2

Interpreting the charge distribution in $Be(CH_3)_2$ in terms of two-centre, two-electron bonds results in an ionic character of 15% for each Be-C bond (as $Be^{\delta+}C^{\delta-}$). This estimate of bond ionicity for the Be-C linkage can be compared to the value of 27% computed recently for the Li-C bond in an ab initio calculation on methyllithium (60). The trend to increasing covalent character for beryllium compounds is also reflected in the overlap populations, the increase being ≈0.2e in going from Li-C to Be-C.

To further investigate the energetics of beryllium alkyl systems, STO-3G calculations were executed on the dimer of $HBeCH_3$ in a geometry with the methyl groups bridging the beryllium atoms as shown schematically by (2).

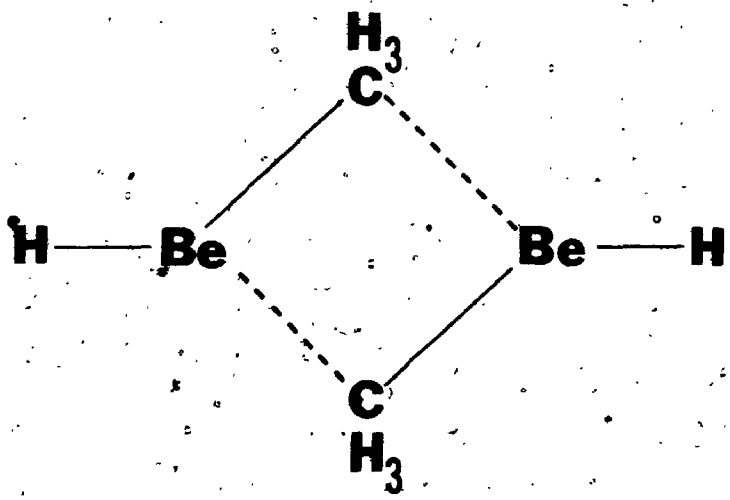

(2)

By analogy with the X-ray diffraction study of the dimethylberyllium polymer (54), a Be-Be distance of 2.09 Å and Be-C bond lengths of 1.93 Å were assumed. For the methyl groups, the same distances and angles as in the monomers were used and in addition, the hydrogens of one methyl group were

assumed to be staggered with respect to those of the second methyl group. The hydride hydrogens were assumed to lie on the Be-Be axis and in the plane formed by the ring atoms. Be-H distances of 1.33 Å were employed.

The calculated energy of -108.3159 a.u. for $(HBeCH_3)_2$ corresponds to a species which is 4.3 kcal mol^{-1} less stable than two monomers. Although optimization of the dimer geometry would probably yield a small positive dimerization energy, such calculations were not executed since the overall magnitude of the dimerization energy will probably be dominated by the change in correlation energy.[1] It is clear however, that the dimerization of beryllium alkyls is much less energetically favourable than for the corresponding lithium alkyls.[2]

The atom-atom overlap populations and gross atomic populations for $(HBeCH_3)_2$ and $HBeCH_3$ are compared in Tables III-5 and III-6, respectively. Several points should be noted from these tables. First, the positive value for the Be-Be overlap population is indicative of substantial covalent metal-metal bonding. Second, the total beryllium-carbon overlap population decreases on dimerization suggesting covalent interactions are not important in dimerization and, third, the electron density on both the beryllium and

---

[1] See also the changes in correlation energy calculated by Ahlrichs for the polymerization of BeH_2 (61).

[2] The dimerization energy for $LiCH_3$ has been computed to be +35 kcal mol^{-1} with the STO-3G basis set (60).

TABLE III-5

Atom-Atom Overlap Populations in $(HBeCH_3)_2$ and $HBeCH_3$

Atom Pair	Monomer	Dimer	Change
Be-C[a]	0.7814	0.7446	-0.0368
C-H (avg)	0.7601	0.7501	-0.0100
H-Be	0.8175	0.8283	+0.0108
Be-Be	—	0.3222	+0.3222
C-C	—	-0.0224	-0.0224

[a]Be-C population is the sum of Be_1-C_1 and Be_1-C_2 interactions.

TABLE III-6

Gross Atomic Populations in $(HBeCH_3)_2$ and $HBeCH_3$

Atom	Monomer	Dimer	Change
Be	3.7139	3.7316	+0.0177
C	6.4303	6.4828	+0.0525
H(Be)	1.1530	1.1669	+0.0139
H(C)	0.9012	0.8729	-0.0283

carbon atoms increases on dimerization, in contrast to the more ionic methyllithium system in which the lithium atom becomes more positive and the carbon atom more negative on dimer formation (60).

Thus, as expected from consideration of the relative electronegativities of lithium and beryllium, beryllium alkyls exhibit a lower degree of ionicity than do the lithium alkyls. In addition, the increase in covalent character in going from lithium to beryllium results in improved stability for the monomeric forms.

(c) Aminoberyllium Compounds

For the amino derivatives of beryllium, even less is known experimentally than for the alkyl compounds. Most are dimeric or trimeric in solution; only one derivative, bis(di(trimethylsilyl)amino) beryllium, is found in monomeric form (62), presumably because steric crowding prevents association. In contrast to the alkyl compounds, considerable π-bonding is expected in the amino derivatives through donation of the nitrogen lone pair electrons to the beryllium p_π orbital. The observation of a planar configuration about nitrogen in several derivatives (62,63) has been used as evidence for extensive dative π-bonding. In addition, the nitrogen lone pair electrons are available for σ-bonding to the beryllium atom of a second aminoberyllium molecule and their donation in this fashion is anticipated to lead to a relatively large dimerization energy.

Preliminary STO-3G calculations with the exponents listed in Table III-1 established that monomeric $HBeNH_2$ was planar and indicated that the NBeH angle was 180°. Assuming an HNH angle of 112°, optimum values of 1.33, 1.53, and 1.04 Å were determined for the H-Be, Be-N and N-H bond distances, respectively. The total energy for this geometry is calculated to be -69.96264 a.u.. Removal of the beryllium $2p_\pi$ orbital perpendicular to the molecular plane results in a loss of stability of 35.2 kcal mol^{-1}; the π-bonding with the other beryllium $2p_\pi$ orbital is relatively unimportant, contributing only 2.4 kcal mol^{-1} to the total energy.

Examination of the SCF wavefunction in Table III-7 reveals that the highest occupied molecular orbital is the partially delocalized nitrogen lone pair. The predicted ionization potential of 9.6eV for removal of an electron from this orbital is only slightly less than the value of 9.7eV predicted for NH_3 with the STO-3G basis set. Both the overlap populations given in Table III-8 and the population analyses given in Table III-9 indicate significant sharing of the nitrogen lone pair. In particular, the orbital populations indicate that 0.35 electrons are transferred from nitrogen to beryllium in the formation of the π bond. The effect of σ-withdrawal/π-donation is more dramatic here than in $HBeCH_3$ partly because of the greater electronegativity of nitrogen and the correspondingly greater ionic character. From the Mulliken population analysis, the ion-

TABLE III-7

SCF Wavefunction For $HBeNH_2$

Molecular Orbital (C_{2v})	ATOMIC ORBITAL[a]													Orbital Energy (a.u.)
	H_1	Be					N					H_2	H_3	
	1s	1s	2s	$2p_x$	$2p_y$	$2p_z$	1s	2s	$2p_x$	$2p_y$	$2p_z$	1s	1s	
$1a_1$	-.0022	.0001	-.0046			-.0074	.9937	.0317			-.0001	-.0054	-.0054	-15.4129
$2a_1$	-.0040	.9920	.0310			-.0012	-.0011	-.0001			-.0036	-.0017	-.0017	-4.5445
$3a_1$	.0092	-.0523	.0423			.0459	-.2247	.7989			.0492	.1653	.1653	-1.0752
$1b_2$					.0643					.6092		.3904	-.3904	-0.6089
$4a_1$	.0783	-.1472	.2892			.2040	-.0400	.1711			-.6831	-.2469	-.2469	-0.5403
$5a_1$	-.5986	.1360	-.3235			.3439	-.0126	.0259			-.0941	.0391	-.0391	-0.4358
$1b_1$				-.2958					-.8800					-0.3556
$2b_2$					1.0257					-.1156		-.1941	.1941	+0.1412
$2b_1$				.9942					-.5491					+0.1900

[a] The coordinate system is chosen with the origin at the beryllium atom, the positive z axis coincident with the Be-N bond and the y axis in the plane of the molecule.

TABLE III-8

Atom-Atom Overlap Populations in $HBeNH_2$

Atom Pair	Overlap Population (in e)	
	with p_π	without p_π
Be-N(σ)	0.5779	0.6314
Be-N(π)	0.3134	—
Be-N(total)	0.8913	0.6314
H(Be)-Be	0.8225	0.8197
Be-H(N)	-0.0719	-0.1055
N-H(N)	0.6852	0.7218
H(N)-H(Be)	0.0002	0.0003
H(N)-H(N)	-0.0461	-0.0525

TABLE III-9

Gross Populations for Orbitals and Atoms in $HBeNH_2$

Atom	Orbital	Gross Population (in e)	
		with p_π	without p_π
Be	1s	1.9930	1.9934
	2s	0.6778	0.7251
	$2p_\sigma$	0.6466	0.7007
	total σ	1.3244	1.4258
	$2p_\pi$	0.3530	—
	total atomic	3.6704	3.4192
N	1s	1.9954	1.9951
	2s	1.5695	1.5127
	$2p_\sigma$	1.2957	1.1994
	$2p_\pi$	1.6868	2.0000
	$2p_y$	1.1053	1.0836
	total atomic	7.6527	7.7907
H(Be)	1s	1.1406	1.1418
H(N)	1s	0.7681	0.8241

icity of the Be-N bond is 21%, midway between the values for Be-C and Li-C bonds. As expected, the calculations predict that the NH_2 group carries a substantial overall negative charge even when π-bonding is operative.

As anticipated above, the energy gain accompanying dimerization of $HBeNH_2$ is substantial. An STO-3G calculation on $(HBeNH_2)_2$ using a geometry with the nitrogen atoms bridging, a Be-Be separation of 2.09 Å, and Be-N bond lengths of 1.65 Å[3] predicts a total energy of -140.0219 a.u. or 60.6 kcal mol^{-1} more negative than two isolated monomers. Examination of the overlap populations in Table III-10 and the gross atomic populations in Table III-11 indicates a higher degree of ionicity for this system than for the Be-C dimer. The large increase in Be-N overlap population accompanying dimerization is a result of the involvement of the nitrogen lone pair in σ-bonding rather than π-bonding as in the monomer and the increase of 0.044 in the positive charge on beryllium is indicative of an increased ionic attraction in the dimer. Of particular note is the large negative value for the Be-Be overlap population.

In conclusion it should be pointed out that the calculations presented here, although more reliable and more realistic than the semiempirical methods are intended mainly to indicate trends. Provision for polarization of the bonds, electron correlation, etc., may result in somewhat different

[3]Derived from the X-ray diffraction structure of the bis(dimethylamino)beryllium trimer (63).

values for the numerical quantities.

TABLE III-10

Atom-Atom Overlap Populations in $(HBeNH_2)_2$ and $HBeNH_2$

Atom Pair	Monomer	Dimer	Change
Be-N[a]	0.8913	0.9890	+.0977
N-H	0.6852	0.6960	+.0108
H-Be	0.8225	0.7805	-.0420
Be-Be	—	-0.2665	-.2665
N-N	—	-0.0485	-.0485

[a]Be-N population is the sum of Be_1-N_1 and Be_1-N_2

TABLE III-11

Gross Atomic Populations in $(HBeNH_2)_2$ and $HBeNH_2$

Atom	Monomer	Dimer	Change
Be	3.6704	3.6260	-.0444
N	7.6527	7.6001	-.0526
H(Be)	1.1406	1.2038	+.0632
H(N)	0.7681	0.7851	+.0170

2. Carbonylnitrenes: Structure and Energetics

(a) Introduction

Although nitrenes are generally considered to be high-energy reactive intermediates quite unco-operative to chemical study, a good deal of information about their properties and reactivity has been obtained experimentally. Carbonylnitrenes (1) and carbalkoxynitrenes (2) especially, have been the subject of some careful and well-planned

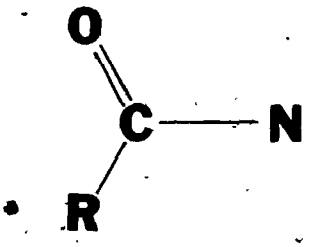

(1)

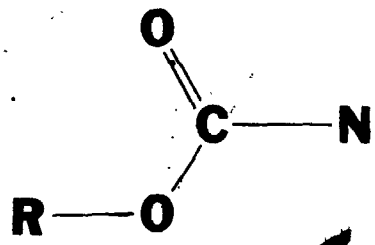

(2)

studies.[1] In particular, it has been found that these nitrenes can be produced both thermally and photochemically, and once formed, react very much like carbenes, their widely studied (65) isoelectronic analogs. That is, nitrenes add to olefins giving aziridines and react with (C-H) bonds giving insertion products.

The experiments of McConaghy and Lwowski with thermally generated carbethoxynitrene (66) indicated that both a singlet and a triplet state were involved in the addition to double bonds. On the basis of Skell's postulate (67)—that the singlet addition should occur stereospecifically and that the triplet addition should occur in a non-con-

[1]For a comprehensive review of the synthesis and reactions of these species, see reference 64, pp. 185-224.

certed, non-stereospecific manner — it was concluded that the nitrene was initially produced in the singlet state and that intersystem crossing to the triplet state occured in competition with addition to the olefin. The triplet state has also been observed in low-temperature esr studies (68) but no experimental information exists concerning the energetics of intersystem crossing, or concerning the electronic structure of either state.

Interestingly, when carbethoxynitrene was produced photochemically from ethyl azidoformate (66), the experimental data indicated that approximately one-third of the nitrene was generated in the triplet state as a primary photolysis product, while the remaining two-thirds was generated in the singlet state. The singlet state was then observed to react with olefins or to cross to the triplet state in the same manner as the thermally generated singlet species.

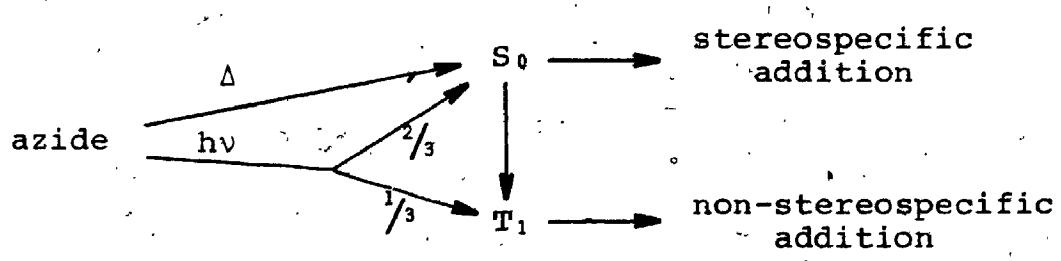

To rationalize this observation, Berry (69) has suggested that some of the nitrene molecules produced in the photolysis are channelled to the triplet state directly, while those remaining are trapped in a secondary minimum on the

singlet potential surface. In addition, Berry speculates that the geometry of the molecule in this secondary minimum could be the novel three-membered ring (3). No direct

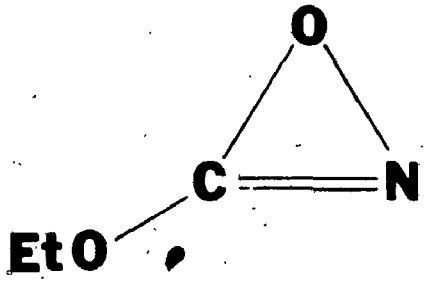

(3)

experimental evidence has been found for this structure but it is interesting to note that it has also been postulated as an intermediate in the photolysis of a nitrile oxide (70):

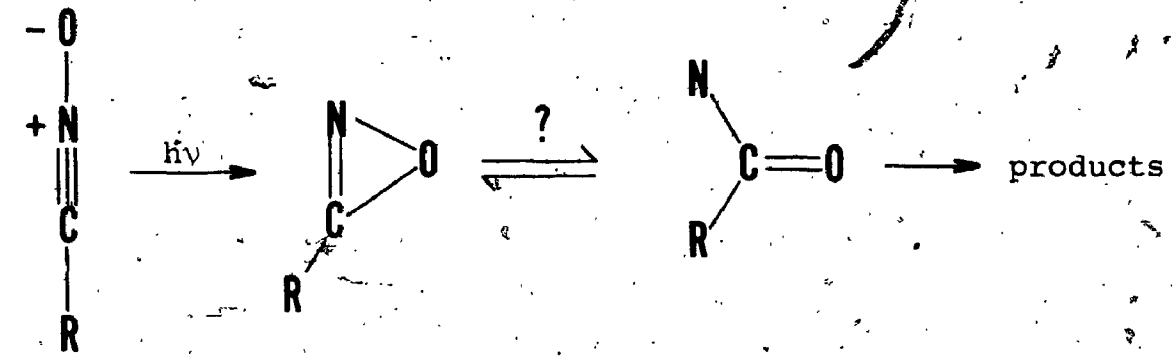

Although the ring isomer is expected to be highly unstable (since involvement of the oxygen lone pair with the double bond makes the system formally anti-aromatic), it is possible that a minimum exists not far in energy from the open form. The calculations reported here explore this intriguing possibility and form the basis for an investigation into the electronic structure of carbonylnitrenes of the type represented by (1) and (2).

(b) The Singlet and Triplet States of Carbonylnitrenes

Both the lowest closed-shell singlet state, S_0, and the lowest triplet state, T_1, of formylnitrene were subjected to a complete geometry optimization under the constraint of C_s symmetry at the STO-3G level. The results are presented in Figures III-1 and III-2.

Note that there is little change in structure between the two states, the only noticeable difference being the length of the C-N bond. This is not unexpected since the change in orbital occupancy between the two states involves orbitals which contribute very little to bonding. From the wavefunction for S_0 given in Table III-12, it can be seen that the highest occupied molecular orbital, 2a'', formally corresponds to the non-bonding π molecular orbital of the analogous allyl system, while the lowest unoccupied molecular orbital, 10a', is primarily a 2p atomic orbital centred on nitrogen and in the plane of the molecule. In T_1, both of these orbitals (see Table III-13) are singly occupied. Even though some reorganization takes place in the π system to localize the non-bonding π orbital completely on the nitrogen atom, the overall change in charge density in going from S_0 to T_1, as measured by the gross orbital and atomic populations given in Table III-14, is small. In addition, the total C=O overlap population remains relatively constant, the change being only about 2% with the change in state. Reorganization of the π system in T_1, is reflected by a lengthening of the C-N bond and by a decrease

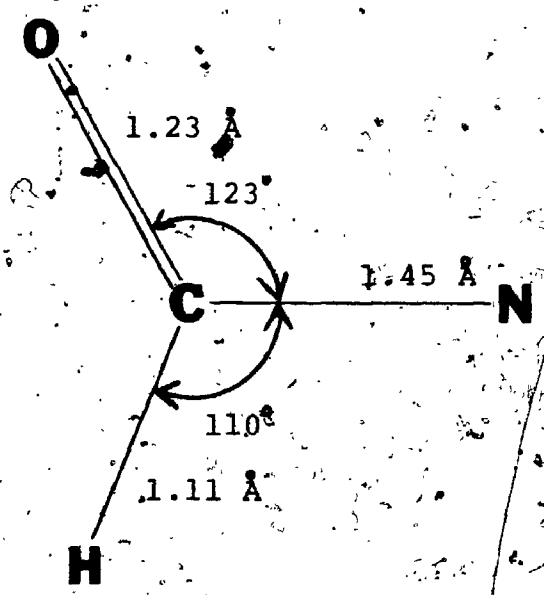

FIGURE III-1

Calculated Optimum Geometry for the Lowest Closed-Shell Singlet State, S_0, of Formylnitrene

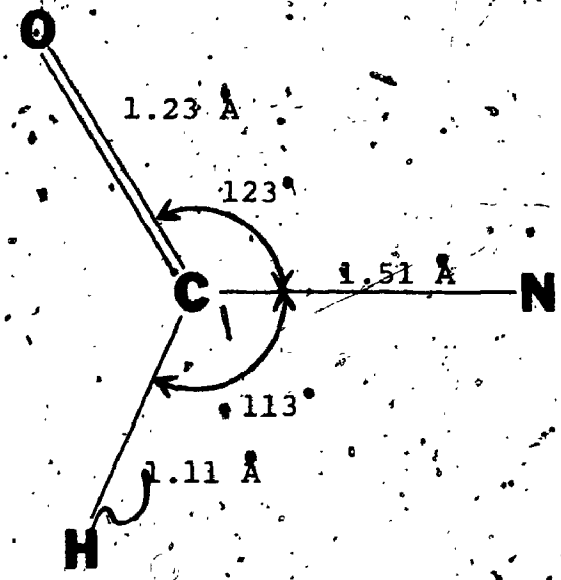

FIGURE III-2

Calculated Optimum Geometry for the Lowest Triplet State, T_1, of Formylnitrene

TABLE III-12

SCF Wavefunction For The S_0 State of Formylnitrene

Molecular Orbital (C_s)	ATOMIC ORBITAL[a]																Orbital Energy (a.u.)
	C					N					O					H	
	1s	2s	$2p_x$	$2p_y$	$2p_z$	1s	2s	$2p_x$	$2p_y$	$2p_z$	1s	2s	$2p_x$	$2p_y$	$2p_z$	1s	
1a'	.0005	-.0070		-.0053	.0034		-.0002		.0005	-.0002	.9943	.0258		-.0046	.0031	.0004	-20.2871
2a'	.0005	-.0056		-.0001	-.0048	.9944	.0243			-.0045		.0002		.0001	.0004	.0001	-15.3964
3a'	.9927	.0320		.0002	.0002	.0005	-.0053		-.0002	.0033	.0002	-.0054		.0013	-.0009	-.0065	-11.1724
4a'	.1314	-.3104		-.1334	.0686	.0346	-.1119		-.0030	.0478	.2113	-.7372		.1340	-.0940	-.0365	-1.3381
5a'	.0891	-.2526		.0926	-.2149	.2045	-.7321		.0055	.1519	-.0778	.2962		-.0115	-.0255	-.0665	-1.0634
6a'	.1405	-.4616		.3053	.1697	-.1019	.4285		.0364	.0945	-.0677	.3008		.2074	.0463	-.3827	-0.7472
7a'	-.0759	.2730		.3788	.1611	.0803	-.3744		.0724	-.2892	.0850	-.4322		-.1763	.5150	-.1860	-0.5795
8a'	.0006	.0093		-.2150	.4034	.0797	-.3929		-.0228	-.4060	-.0667	-.3619		.5729	.0028	.0836	-0.5200
1a''			-.5603					-.4972					-.4849				-0.5074
9a'	-.0051	.0336		.0597	.1413	.0158	-.0868		.0145	-.4552	-.0028	.0166		-.4324	-.7136	-.3267	-0.3483
2a''			-.2010					.8166					-.5546				-0.3340
10a'	.0017	-.0090		-.0571	.0273	.0006	-.0027		.9761	-.0186	-.0113	.0666		-.1137	.1361	-.2057	+0.1634
3a''			.8467					-.3362					-.7078				+0.2835

[a] The coordinate system is chosen with the origin at the carbon atom, the positive z axis coincident with the C-N bond and the y axis in the plane of the molecule.

TABLE III-13

SCF Wavefunction For The T_1 State of Formylnitrene

Molecular Orbital (C_s)	ATOMIC ORBITAL[a]															Orbital Energy (a.u.)
	C					N					O					H
	1s	2s	$2p_x$	$2p_y$	$2p_z$	1s	2s	$2p_x$	$2p_y$	$2p_z$	1s	2s	$2p_x$	$2p_y$	$2p_z$	1s	
1a'	-.0005	.0069		.0052	-.0034		-.0002		-.0004	.0002	-.9943	-.0256		.0046	-.0030	-.0002	-20.3347
2a'	-.0006	.0049		.0001	.0046	.9955	-.0197			.0045		-.0002		-.0002	-.0006	-.0001	-15.3156
3a'	.9927	.0316		.0004	-.0007	.0005	-.0047		-.0002	.0032	.0002	-.0056		.0014	-.0010	-.0065	-11.1612
4a'	.1230	-.2857		-.1316	.0849	.0137	-.0393		-.0009	.0325	.2178	-.7652		.1409	-.0949	-.0335	-1.3463
5a'	-.1566	.4867		-.1481	.1610	-.1311	.4448		-.0057	-.2212	.0893	-.3754		-.0703	.0943	.1963	-0.8748
6a'	.0721	-.2371		.2734	.3483	-.1181	.4421		.0246	-.1188	-.0394	.1868		.2875	.1994	-.3367	-0.6888
7a'	.0547	-.1864		-.4084	-.0969	-.0551	.2198		-.0386	-.0035	-.0986	.5146		.4494	-.4825	.1819	-0.5689
8a'	.0441	-.1713		.1014	-.2180	-.1504	.6566		-.0016	.2089	.0090	-.0589		-.5073	-.4785	-.1963	-0.4463
1a"			-.6087					-.0832					-.6655				-0.4447
9a'	-.0311	.1448		.0571	.2920	.0877	-.4094		.0132	-.5887	-.0018	.0175		-.2679	-.5314	-.2778	-0.3136
2a"			-.0079					-.9754					.2237				-0.0893
10a'	-.0033	.0169		-.0086	-.0179	-.0005	.0016		.9953	.0169	.0072	-.0346		.0664	-.0816	.1090	-0.0820
3a"			.8336					-.2514					-.7421				+0.2445

[a] See footnote a, Table III-12.

TABLE III-14

Gross Orbital Populations for the S_0 and T_1 States of Formylnitrene

Atom	Orbital[a]	Population (in e)	
		S_0	T_1
C	1s	1.9937	1.9938
	2s	1.1246	1.1435
	$2p_x$	0.9009	0.9207
	$2p_y$	0.9550	0.9161
	$2p_z$	0.8580	0.8721
	total atomic	5.8322	5.8462
N	1s	1.9986	1.9988
	2s	1.8905	1.9046
	$2p_x$	1.8615	0.9801
	$2p_y$	0.0333	0.9963
	$2p_z$	1.2396	1.1708
	total atomic	7.0235	7.0506
O	1s	1.9982	1.9982
	2s	1.8741	1.8745
	$2p_x$	1.2376	1.0992
	$2p_y$	1.4365	1.4898
	$2p_z$	1.6823	1.7135
	total atomic	8.2287	8.1752
H	1s	0.9155	0.9280

[a]See footnote a, Table III-12.

in the C-N π overlap population from 0.0735e in S_0 to 0.0312e in T_1. Since both of these values are low compared to the value of ≈0.3e calculated for the C=O π bond, it is reasonable to visualize the C-N bond as a single bond in both states.

Total energies for the T_1 and S_0 states at their optimum geometries are calculated to be -165.4672 a.u. and -165.3932 a.u., respectively. The triplet energy was calculated using Roothaan's open-shell method (8), and 2X2 CI between the ground state configuration and that formed by a double excitation from the non-bonding π molecular orbital to the vacant 2p atomic orbital on nitrogen was included in the calculation of the singlet energy to compensate for the automatic correlation of the unpaired electrons in the triplet state. The singlet-triplet separation is calculated to be 63.1 kcal mol^{-1}, in considerable disagreement with the value of 15 kcal mol^{-1} computed recently for formylnitrene by Alewood, Kazmaier and Rauk (71). In the latter calculation, however, the triplet energy was estimated using the closed-shell eigenvectors of S_0, which, in this instance is a particularly poor procedure. The 2a'' orbital of the singlet state, as previously mentioned, is formally the allyl-type non-bonding molecular orbital and is delocalized over the carbonyl group to a considerable extent.[2] Thus, removing one electron from this orbital

[2]The delocalization of the 2a'' orbital in the singlet state is illustrated particularly well by examining the

and placing it in the empty p orbital on nitrogen constitutes a charge transfer of the type discussed in Chapter II. The Roothaan method, on the other hand, converges to a solution in which the π bonding orbital, 1a'', is localized on the C=O group and both singly-occupied orbitals are localized on nitrogen. This, incidently, agrees with indications from the esr work on carbethoxynitrene (68) that the unpaired electrons are not extensively delocalized onto the carbonyl group in the triplet state.

There is, however, some reason to believe that the singlet-triplet separation of 63.1 kcal mol^{-1} computed here is too large. Previous experience with calculation of the corresponding energy difference in CH_2 (72,73) suggests that a minimum basis set does not describe the singlet state as well as it does the triplet state. In particular, for CH_2, use of the STO-3G basis set with 2X2 CI for the singlet state and with Roothaan's method for the triplet state yields a separation of 29 kcal mol^{-1}, whereas more sophisticated SCF calculations using a much larger basis set including d polarization functions on the carbon and p functions on the hydrogens and with a much greater degree of configuration interaction predict a value of 11.0

---

gross orbital populations for the $2p_\pi$ atomic orbitals contributing to this molecular orbital. If the MO is occupied by one electron, as is the case when the closed-shell orbitals are used for the triplet state, the populations of the carbon, nitrogen and oxygen $2p_x$ atomic orbitals are 0.0367, 0.6368, and 0.3265e respectively. The corresponding populations when the Roothaan method is used are 0.0008, 0.9510 and 0.0482e.

±2 kcal mol^{-1} (73). Two other high-level ab initio methods, GVB-CI (generalized valence bond theory with configuration interaction) and IEPA-PNO (independent electron pair approach with pair natural orbitals), predict separations of 11.5 (74) and 9.2 kcal mol^{-1} (75) respectively. All three values are in good agreement with the most recent experimental determinations of 8-8.5 (76) and 9 kcal mol^{-1} (77). Since CH_2 is isoelectronic with the parent nitrene NH, the "error" in the present calculations is probably in the same direction and of the same magnitude as for CH_2. Thus, it is predicted that more refined calculations would predict a singlet-triplet separation of approximately 45 kcal mol^{-1} for formylnitrene.

It is interesting to note that the calculations predict that the open-shell singlet state, S_1, (i.e., with the same electron configuration as the triplet state but with spins paired) lies 48.5 kcal mol^{-1} above the triplet state. This is expected to be somewhat of an overestimation, since it is computed by assuming that the optimum triplet state geometry and the triplet wavefunction are both suitable for this singlet state. The error is not expected to be appreciable, since these two states are built from the same electron configuration, but it is probably large enough to place S_1 below S_0. Thus, it is conceivable that two singlet states are involved in the reactions of carbonylnitrenes. Verification of this point experimentally appears to be difficult, however, since recent ab initio calculations

by Haines and Csizmadia (78) on the addition of NH to ethylene have indicated that the S_1 and T_1 states should behave very much alike. Specifically, the calculations have demonstrated that the lowest energy pathway for addition when either S_1 or T_1 is involved leads to loss of stereospecificity in the product aziridine, while the addition of S_0 nitrene occurs with retention of stereochemistry. This is also supported by the theoretical work of Hoffmann (79) on the analogous carbene-ethylene reactions. The present calculations, therefore, suggest that the non-stereospecific addition of carbonylnitrenes to olefins as reported by McConaghy and Lwowski (66), could arise from either the ground state triplet or from the open-shell singlet state.

The calculations of Alewood et al. (71) indicate that alkyl substitution in formylnitrene has only a small effect on the S_0-T_1 separation, but that alkoxy substitution could have a major effect. In particular, it was found that for acetylnitrene (4), the S_0-T_1 separation is reduced by only 3 kcal mol^{-1} from the value obtained for formylnitrene, while for carbhydroxynitrene (5), it is reduced by 38 kcal

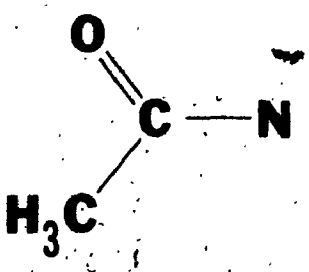

(4)

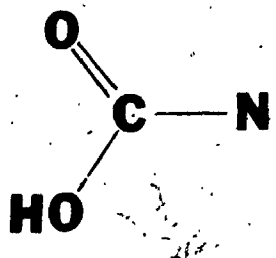

(5)

mol^{-1} so that the singlet is predicted to be the ground state, lying 23 kcal mol^{-1} below T_1. Although the authors

point out that this separation would decrease if an SCF calculation, accompanied by geometry optimization, was carried out for the triplet state, it was concluded that carbalkoxynitrenes may have singlet ground states. However, since the esr work on carbethoxynitrene (68) has definitely shown that this molecule has a triplet ground state, this conclusion is questionable and worthy of further investigation as reported below.

In view of the results for formylnitrene, a complete geometry optimization for both the S_0 and T_1 states of carbhydroxynitrene was not judged to be economical. Instead, the optimum geometries determined for formylnitrene were used (see Figures III-1 and III-2). The geometry of the (O-H) group[3] was chosen to be the same as that determined by electron diffraction for the (O-H) group in formic acid (80). Total STO-3G energies are calculated to be -239.2466 a.u. and -239.3504 a.u. for the singlet and triplet states, respectively. The singlet-triplet separation is thus calculated to be 65.1 kcal mol^{-1}, very close to the value of 63.1 kcal mol^{-1} computed for formylnitrene. The comments regarding the formylnitrene wavefunction also apply to this system; there is little change in overall charge density or overlap population between the S_0 and T_1 states and the unpaired electrons in T_1 are localized on

[3]That is, the OH group was assumed to be co-planar with the rest of the molecule, and with R(C-O) = 1.36 Å, R(O-H) = 0.97 Å and angle (COH) = 105°. As indicated in (5), the OH group was assumed to be cis relative to C=O.

the nitrogen atom. Thus, any error in the S_0-T_1 separation is expected to be much the same in both formylnitrene and carbhydroxynitrene. It should also be pointed out that the use of the closed-shell method along with the basis set used here predicts (incorrectly) S_0 to be the ground state lying 34 kcal mol^{-1} below T_1. Interaction of the hydroxyl-oxygen lone pairs with the π system in S_0 causes a greater delocalization of the nitrogen π lone pair electrons than in formylnitrene, resulting in an even worse representation of the triplet state by the singlet wavefunction. In summary, the S_0-T_1 split is not altered appreciably by substitution of -OH for -H in formylnitrene if SCF wavefunctions for both states are employed. The contrary prediction in the calculations reported by Alewood et al. is due to their use of the S_0 wavefunction for T_1 and their incorrect assumption that the "error" in T_1 so introduced is not affected by substitution.

(c) Oxazirene

Interest in oxazirene, the ring isomer of formylnitrene, lies in determining its ground state energy relative to the energy of the S_0 state of formylnitrene. If this determination is to be done accurately, care must be taken to ensure that both isomers are treated on an equal basis and that the changes in electronic structure which occur during the isomerization are described adequately. In this context, there are two major concerns; namely, the

change in correlation energy accompanying the formation of the bond between the oxygen and nitrogen atoms, and the increase in strain energy associated with closing the ring.

The correlation energy problem arises from the mixing of the oxygen in-plane lone pair orbital with the vacant 2p orbital on the nitrogen atom. Since the occupied spatial orbital increases in size because of this mixing, the electrons will be on the average further apart. Thus, the error from neglecting electron correlation can be expected to be somewhat greater in oxazirene than in formylnitrene. The simplest way to correct for this change in correlation energy is to allow the bonding and antibonding combinations of these orbitals to interact through configuration interaction. Molecular orbitals 9a' and 10a' are localized representations of the atomic orbitals in the open form and correlate smoothly with the σ and σ^* orbitals of the closed form. Thus, 2X2 CI between the ground configuration and the doubly excited configuration formed by the two-electron excitation from 9a' to 10a' introduces the proper electron correlation into the state wavefunction.

As for the prediction of strain energy of small rings, the reliability of the STO-3G method is not known. Calculations reported by Pople and coworkers (19) indicate that the energies of cyclic relative to acyclic hydrocarbons are overestimated, but extension of this prediction to the present case cannot be justified in view of the other errors inherent in the method. For instance, use of the STO-3G

basis has been found (16) to favour single bonds over double bonds in hydrocarbons and although there is little data on the corresponding carbon-oxygen or carbon-nitrogen systems, it seems likely that such errors will also occur in these systems. This particular problem can be overcome by using the extended 4-31G basis set. Strain energy is still overestimated (19) but Pople and coworkers (15,20) have shown that the greater degree of flexibility afforded by this basis set effectively eliminates the errors associated with changing bond types. In addition, the larger basis set leads to a total energy closer to the Hartree-Fock limit so the use of configuration interaction will not be as crucial in describing the oxygen-nitrogen σ bond.

Complete geometry optimization for both isomers with the larger basis set is not economical at present. Consequently, the theoretical geometry of oxazirene, depicted in Figure III-3, was determined using the STO-3G basis set including the CI discussed above and assuming C_s symmetry. Configuration interaction is found to have a negligible effect on the predicted structure of formylnitrene, but has a rather dramatic effect for oxazirene. In particular, the inclusion of CI leads to the prediction of an unusually long oxygen-nitrogen bond distance of 1.69 Å, whereas the single-determinant formalism predicts a much shorter distance of 1.55 Å. To check that this finding was realistic and not a defect of the CI procedure, this particular bond length was also optimized using the 4-31G basis, both with

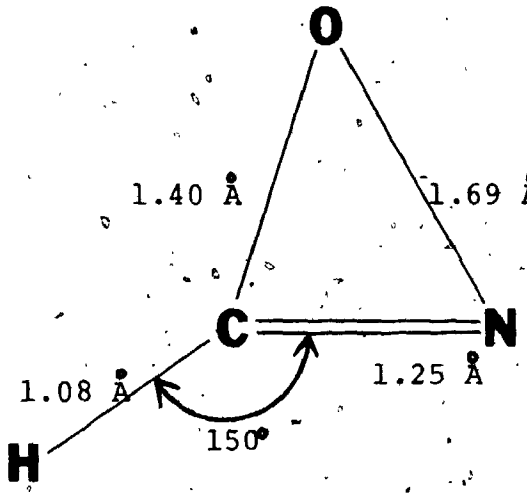

FIGURE III-3

Calculated Optimum Geometry for Oxazirene

and without CI. In each case the bond is predicted to be long; 1.75 Å without CI and 1.74 Å with CI. Thus, the effect of CI is somewhat smaller when used in conjunction with the extended basis set.

Total single-determinant 4-31G energies are computed to be -167.3430 a.u. and -167.3238 a.u. for formylnitrene and oxazirene respectively when each molecule is at its optimum STO-3G (with CI) geometry. The isomerization energy is thus predicted to be 12.0 kcal mol^{-1}, with the acyclic form lower in energy. Use of CI reverses the order of stability, yielding total energies of -167.3432 a.u. and -167.3511 a.u. for the acyclic and cyclic species, respectively, resulting in a calculated isomerization energy of 5.0 kcal mol^{-1}.

It is important to point out here, that in previous calculations with this basis set on the analogous hydrocarbon systems (15), the energies of cyclic relative to acyclic molecules have been overestimated. Specifically, Pople and coworkers have found that cyclopropene is predicted to be 15.4 kcal mol^{-1} too unstable with respect to allene, and cyclopropane 5.8 kcal mol^{-1} too unstable relative to propene. Configuration interaction has not been used in these calculations but it has been found (81) that augmenting the basis set with polarization functions eliminates most of the discrepancy and gives isomerization energies in good agreement with experiment. For this reason it is suggested that the isomerization energy of

12.0 kcal mol^{-1} for the formylnitrene-oxazirene interconversion is an overestimation and that the value obtained by including CI in the calculation is the better estimate. This value however, may involve errors of a few kilocalories per mole and should not serve as anything more than an indication that the isomers are of comparable energy.

(d) Barrier to Isomerization

Given that formylnitrene and oxazirene are of approximately equal energy, it would be interesting to determine whether a substantial barrier exists to their interconversion or whether it is possible for them to exist in thermal equilibrium. Unfortunately, the computational facilities for studying the isomerization reaction in great detail are not yet available and consequently some approximations must be used. Probably the least severe approximation used for this study is to assume that the movement of nuclei from their positions in formylnitrene to those in oxazirene follows the least-motion pathway illustrated schematically in Figure III-4. (Also shown are the points at which STO-3G-CI calculations have been performed.) The total energies at each point are given in Table III-15 and, in the upper part of Figure III-5, these energies are plotted as a function of reaction coordinate. The solid line through the points is a least-squares fit fourth-degree polynomial which peaks just slightly to the nitrene side of the geometrical mid-point of the reaction. At the maximum, the energy is estimated to be -165.3658 a.u. which exceeds that

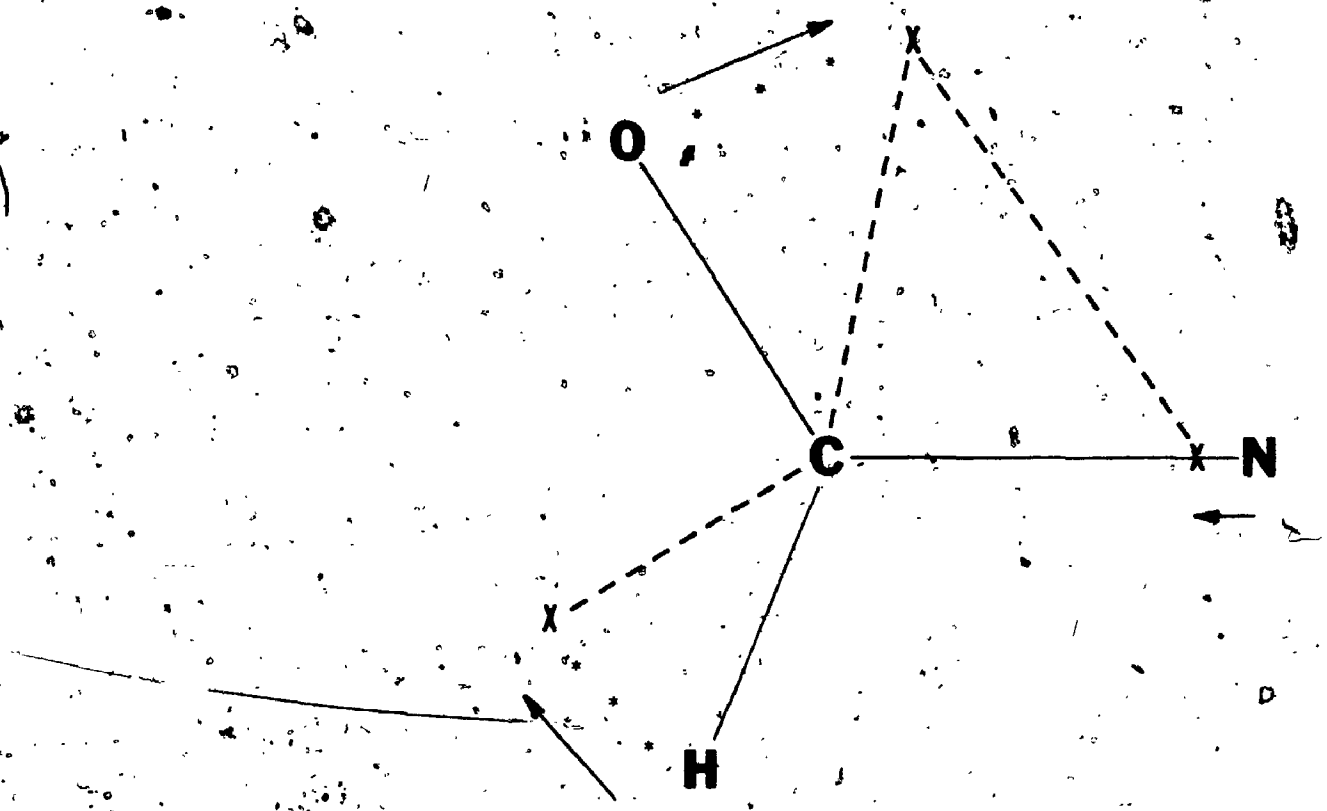

FIGURE III-4

Least Motion Pathway for the Formylnitrene-Oxazirene Isomerization

TABLE III-15

Total STO-3G-CI Energy At Indicated Points on the Formylnitrene-Oxazirene Potential Surface

Geometrical Configuration	Energy
formylnitrene	-165.3907
¼ displacement	-165.3781
mid-point	-165.3680
¾ displacement	-165.4099
oxazirene	-165.4490

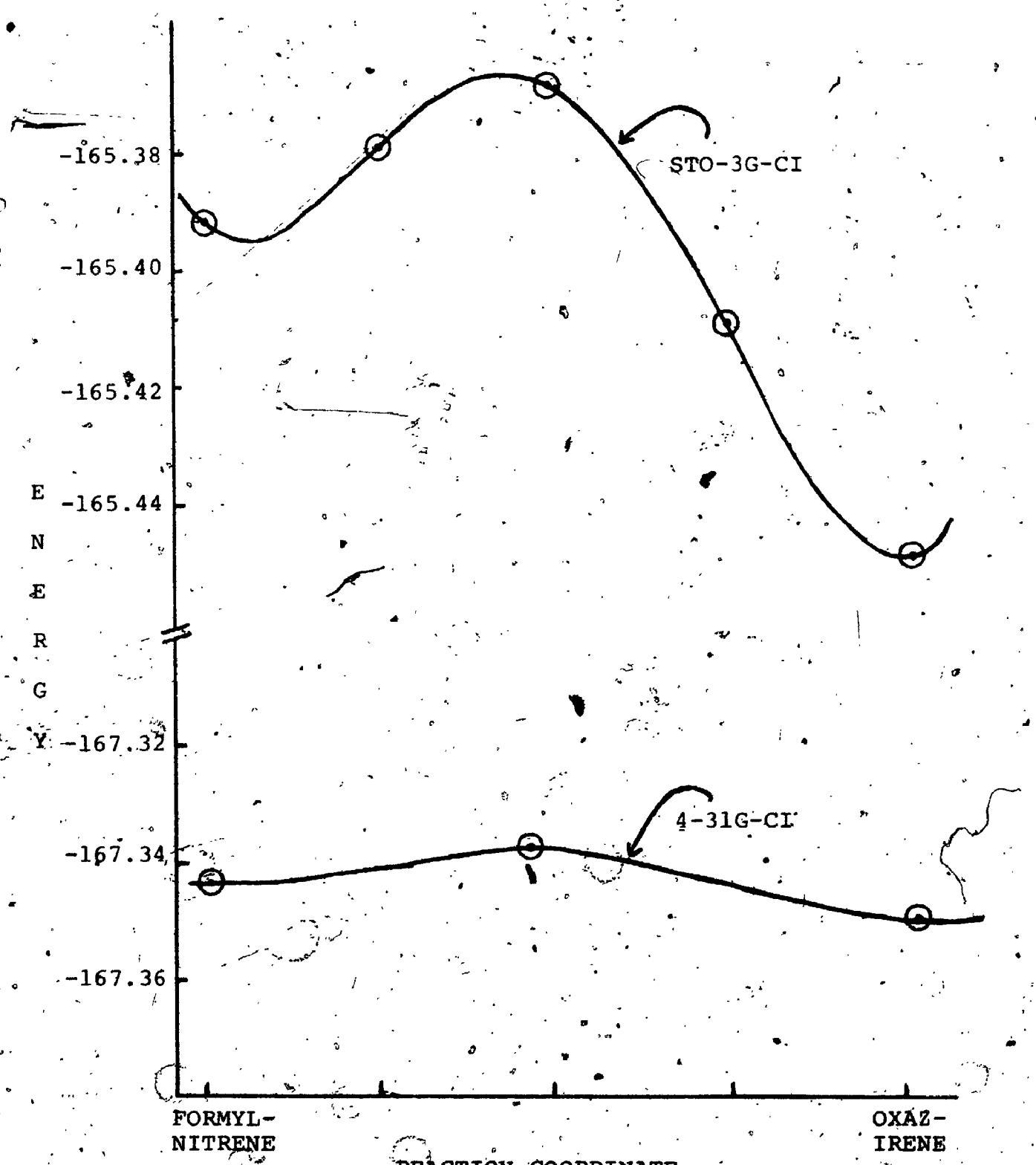

FIGURE III-5

Potential Energy Curves for the Formylnitrene-Oxazirene Isomerization

of formylnitrene by 15.6 kcal mol^{-1} and that of oxazirene by 52.2 kcal mol^{-1}.

Although the inadequacies of the STO-3G basis set cast some doubt on the accuracy of these values, it is not likely that the description of the interconversion deviates far from this model. To try to estimate the barrier height more precisely however, a 4-31G calculation was carried out at the reaction coordinate corresponding to the energy maximum in the STO-3G-CI pathway. Inclusion of CI in the calculation yields a total energy of -167.3381 a.u. which is 8.2 kcal mol^{-1} above the total energy of oxazirene and only 3.2 kcal mol^{-1} above that of formylnitrene. The approximate potential curve is plotted in the lower part of Figure III-5. Given that the reaction path assumed for the calculations is only an approximation to the lowest-energy route, these results indicate that there is effectively no barrier to the interconversion of formylnitrene and oxazirene. Obviously more detailed calculations are required to determine the optimum energy surface but it is unlikely that this would result in the prediction of a substantial thermal barrier to isomerization.

(e) Conclusions

The absence of an energy barrier between the cyclic and acyclic forms of carbonylnitrenes tends to discredit Berry's suggestion (69) that oxazirenes can act as efficient traps for singlet carbonylnitrenes and thus prevent the

direct formation of triplet nitrene in the photolysis of azides. The oxazirene isomer may still play an important role in the chemistry of carbonylnitrenes, however. In particular, since the ground state of oxazirene is predicted to be a singlet while that of formylnitrene is a triplet, the S_0 and T_1 potential surfaces must cross for a geometry intermediate between the open and closed forms. Intersystem crossing between S_0 and T_1 is expected to be a relatively efficient process near this intersection since, as has been shown experimentally for aromatic hydrocarbons (82), the rate of intersystem crossing is extremely sensitive to the energy difference between the states. Thus isomerization in the S_0 state from the acyclic to the cyclic form (which is predicted to be a facile process because of the flat potential energy surface) should provide a pathway to the triplet ground state of the nitrene.

A second factor which must be considered in explaining the results of the photolysis experiments of McConaghy and Lwowski (66) is the prediction that the open-shell singlet state, S_1 of carbonylnitrenes lies close in energy to S_0. As was pointed out earlier, the calculations reported by Haines and Csizmadia (78) indicate that the addition products derived from S_1 and T_1 nitrenes should be identical. Thus, the non-stereospecific addition products which are assumed to arise from the T_1 state of carbethoxynitrene in the photolysis of the corresponding azide may, in fact, arise from S_1. Since it has also been shown that the trip-

let state of the azide is not involved in the production of the nitrene (66), the possibility that S_1 is a primary photolysis product must also be considered.

In summary, the results presented here support the major conclusions drawn from the experimental work on carbonylnitrenes — that both a singlet state and a triplet state are involved in the reactions of these compounds and that the triplet state lies lower in energy. There are indications from the calculations however, that geometrical isomerization in the singlet state affects the rate of intersystem crossing to the triplet state and that a second singlet state of reactive character similar to the triplet state may be important in the chemistry of these nitrenes. Unfortunately no facile explanation of all the experimental results in terms of the present calculations seems obvious at this time.

3. Singlet and Triplet States of Aminonitrenes

(a) Introduction

The chemistry of aminonitrenes (1,1-diazenes) has received some attention recently (83,84), due to the synthetic utility of these species in the preparation of aziridines. A considerable amount of information concerning the reactivity of the "nitrene nitrogen" has been collected by Rees and co-workers (85-89, see also ref. 90) via experiments using phthalimido nitrene (1) and related compounds. In particular, these compounds are found to add stereospecifically to olefins, producing aziridines (2). In addition, if dienes are employed as the acceptors, the addition occurs exclusively in the 1,2 manner as shown:

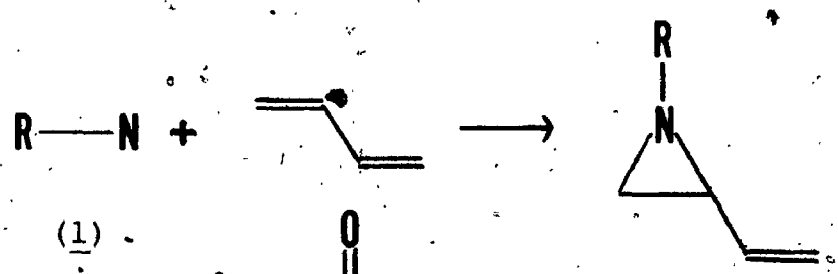

(1)

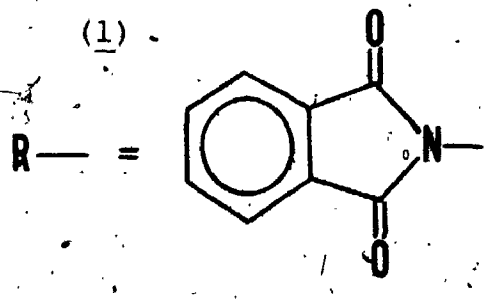

(2)

Since the product composition does not change when the olefin concentration is reduced to relatively low levels, it has been concluded that the reaction involves the ground state of the nitrene. The stereospecificity of the addition and the observation that the yields of the aziridine increase when olefins substituted by electron-withdrawing groups are used, are both consistent with a nucleophilic

singlet state as the reacting species.

In contrast, most other types of nitrenes, including carbonylnitrenes, discussed earlier, are found to have triplet ground states. The distinction in the case of aminonitrenes is thought to be due to the presence of the lone pair π electrons of the "amino nitrogen". Delocalization of these electrons onto the nitrene nitrogen should stablize the singlet state, through the classical valence bond structure (3b), and should destablize the triplet state.

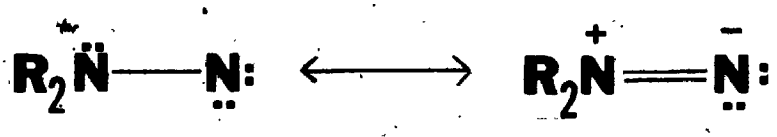

(3a) (3b)

This effect is considered to be important enough to reverse the usual order of stability of the singlet and triplet states (85,89,91).

Unfortunately there exists, at present, very little quantitative information from either physical measurements or from accurate quantum mechanical calculations regarding the bonding and geometries of the low-lying states of either the (unknown) parent compound H_2NN or its simple derivatives. Although semiempirical calculations by the INDO (91) and GNDO/2 (92) methods for H_2NN have been reported, their reliability in this context is questionable, especially since the singlet-triplet separation (91) of more than 1 a.u. (i.e., > 630 kcal mol^{-1}) is obviously much too large. An *ab initio* calculation reported by Wagnière (93) after completion of this work, indicated that the triplet state was

2-4 kcal mol^{-1} lower in energy than the singlet state but this latter calculation did not include geometry optimization for either state. The calculations presented here were undertaken to obtain a better estimate of the singlet-triplet separation, to find the effect of substituents on this separation and to determine the optimum geometry of the parent molecule.

(b) The Lowest Triplet State

Simultaneous optimization of the geometric variables for the lowest triplet state of H_2NN yields a nonplanar, almost tetrahedral structure of C_s symmetry with a relatively long nitrogen-nitrogen bond:

$R_{NN} = 1.43_6$ Å HNN = 107.5°

$R_{NH} = 1.03_4$ Å HNH = 107.5°

The total energy for this pyramidal shape, calculated with the STO-3G basis set, using Roothaan's open-shell procedure (8), is -108.5889 a.u.. This energy is 7.6 kcal mol^{-1} more negative than that for the optimum planar triplet (in which the N-N distance contracts to 1.40 Å); this inversion barrier should be regarded as an upper limit, given that Pople and co-workers have found that the NH_3 barrier is greatly over-estimated using an STO-3G basis set (17). Both the quasi-tetrahedral shape and the Mulliken population analysis (see Table III-16) for triplet amidonitrene are consistent with the valence bond representation (4). In particular, the unpaired spin is almost completely localized (96%)

TABLE III-16

Gross Orbital Populations for Singlet and Triplet H_2NN

Atom	Orbital[a]	Population (in e)	
		Singlet	Triplet
N_{amino}	1s	1.9951	1.9956
	2s	1.4406	1.5914
	$2p_x$	1.6393	1.6295
	$2p_y$	1.1142	1.0681
	$2p_z$	1.0922	1.0656
	total atomic	7.2814	7.3502
$N_{nitrene}$	1s	1.9982	1.9988
	2s	1.8327	1.8938
	$2p_x$	0.3607	1.0607
	$2p_y$	1.9270	1.0102
	$2p_z$	0.9849	1.0337
	total atomic	7.1035	6.9972
H	1s	0.8076	0.8263

[a]The origin of the coordinate system was chosen at the amino nitrogen with the z axis coincident with the N-N bond, the y axis lying in the plane of the H_2N unit, and the x axis mutually perpendicular to y and z. The optimum molecular geometry for the state in question is used in both cases.

(4)

on the nitrene nitrogen atom and the symmetry-allowed delocalization of the amino lone pair into the quasi-π $2p_x$ orbital of the nitrene nitrogen occurs only to the extent of 0.06e. Similarly the population of 1.01e for the nitrene nitrogen $2p_y$ orbital is very close to the idealized value expected from (4). Thus the nitrogen-nitrogen linkage in the triplet is almost exactly that of a single σ bond.

(c) The Lowest Singlet State

For reasons given in the introduction to this section, it is anticipated that the lowest singlet state of aminonitrene corresponds to the closed-shell species, as illustrated by the "idealized" structure (5), rather than to the open-shell configuration (6). The triplet (7), however, correlates with the $^3(n\pi^*)$ state of the isoelectronic mole-

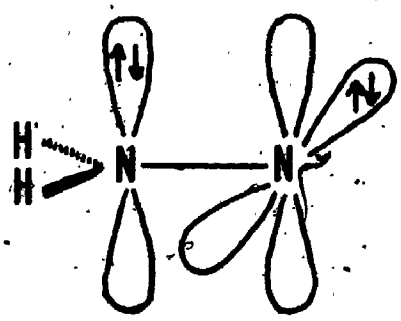

(5)

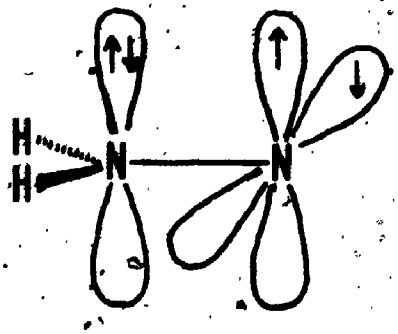

(6)

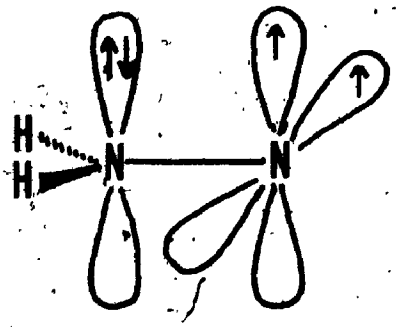

(7)

cule formaldehyde, in which the splitting between the singlet

and triplet ($n\pi^*$) states is rather small (33), an observation which suggests that the singlet (6) does not lie far above the triplet. An STO-3G calculation (using the triplet wavefunction as was done for formylnitrene in the previous section) however, predicts that the splitting is rather large for H_2NN — approximately 48 kcal mol^{-1} for the pyramidal geometry, compared to ≈13 kcal mol^{-1} calculated for H_2CO. The difference between H_2NN and H_2CO is due to the fact that the unpaired π electron in H_2NN is localized heavily on the nitrene nitrogen and thus the $n\pi^*$ exchange integral and the singlet-triplet separation is substantial. The corresponding unpaired electron density in H_2CO is localized largely on the carbon atom, thus yielding a much smaller $n\pi^*$ exchange integral and singlet-triplet split. Thus, it is reasonable to exclude the open-shell configuration (6) from further consideration.

Optimization of the geometrical variables for the closed-shell singlet (5) was carried out with the STO-3G basis set under the assumption that the molecule had C_s symmetry in this state. Configuration interaction between the ground configuration, $\ldots(\pi)^2(n)^2(\pi^*)^0$, and the doubly-excited configuration, $\ldots(\pi)^0(n)^2(\pi^*)^2$, was included to aid the description of the nitrogen-nitrogen bond. The optimum structure is found to be planar with C_{2v} symmetry and a nitrogen-nitrogen bond length similar to the double bond value of 1.25 Å predicted for diimide (42):

$R_{NN} = 1.27_6$ Å angle HNN = 124°

$R_{NH} = 1.04_1$ Å

These values are in good agreement with those of an earlier ab initio calculation for planar singlet H_2NN by Allen and co-workers (1.282 Å, 1.003 Å, 122° respectively) (94) and with the semiempirical INDO (91) and CNDO/2 (92) calculations. Both the short NN distance and the requirement for a planar geometry are indicative of a relatively strong coordinate π bond between the nitrogens, even though the transfer of charge from the amino lone pair to the vacant $2p_\pi$ orbital of the nitrene nitrogen amounts to only 0.36e. As discussed by Baird and Datta (95), the existence of a strong coordinate π bond does not require near-equal sharing of the electron pair; thus, the 0.36e transfer here yields a π overlap population which is 73% of the maximum "covalent" value (i.e., the value which would be achieved if the electron pair was shared equally). The π bonding MO (predicted ionization potential 12.3eV) is not the highest-occupied orbital but rather it is the second highest; the highest-occupied MO (predicted ionization potential 7.6eV) corresponds to an in-plane orbital of b_2 symmetry which is almost completely localized on the nitrene nitrogen. The energetic stability of this lone pair orbital is significantly lower than that in ammonia (predicted ionization potential 9.7eV for NH_3).

Overall, the polarity of the nitrogen-nitrogen multiple linkage agrees qualitatively with that anticipated from resonance between the two important valence bond structures (3a) and (3b) for the singlet, since the transfer of

π electron density from the amino to the nitrene nitrogen exceeds the back transfer of σ electron density in the opposite direction. The overall charge distribution (Figure III-6) is in apparent disagreement with this resonance since the amino nitrogen is more negatively charged than is the nitrene nitrogen, however the high electron density at the amino nitrogen is due primarily to the polarity of the N-H bonds.

Finally, it should be noted that the total energy of -108.5470 a.u. for singlet aminonitrene corresponds to a structure which is some 36.4 kcal mol^{-1} less stable than is the isomeric trans-diimide (calculated using 2X2 CI with the same double-excited configurations in both cases). In contrast, the lowest triplet state of H_2NN is predicted to be 46.2 kcal mol^{-1} more stable than is the lowest (twisted) triplet of drimide (42).

(d) Aminonitrene Derivatives

STO-3G calculations for the monomethyl (8), monofluoro (9), and monocarbonyl (10) derivatives of aminonitrene were carried out for both the singlet and triplet states. In all cases, nitrogen-nitrogen bond lengths and amino nitrogen bond angles which are optimum for H_2NN were assumed in the derivatives. All remaining distances and angles in (10) were assumed equal to the experimental values established for formamide (96). The N-C and N-F distances of 1.47 and 1.37 Å respectively, assumed in (8) and

2 2

OF/DE

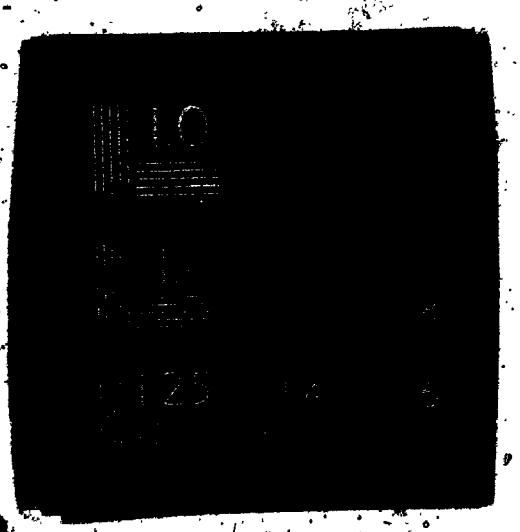

ARC - 574

FIGURE III-6

Gross Atom Net Charges (signed quantities) and Selected Gross π Orbital Populations (in parentheses) for the Lowest Triplet and Singlet States of Aminonitrenes. All quantities are in electron units.

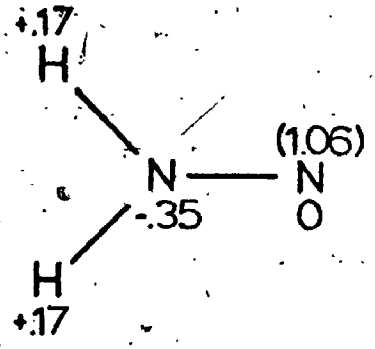

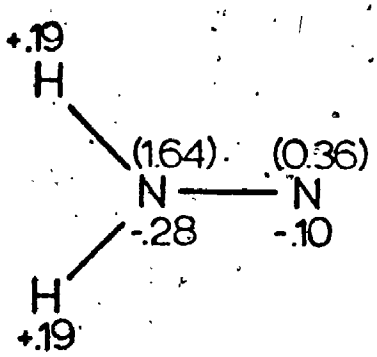

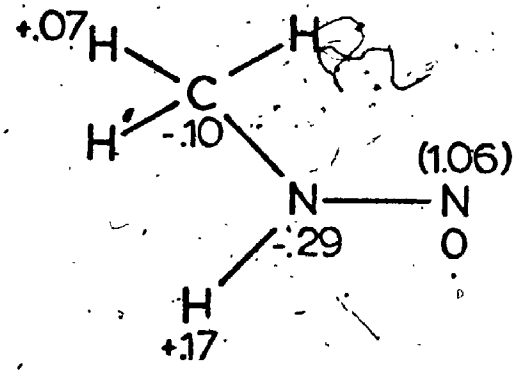

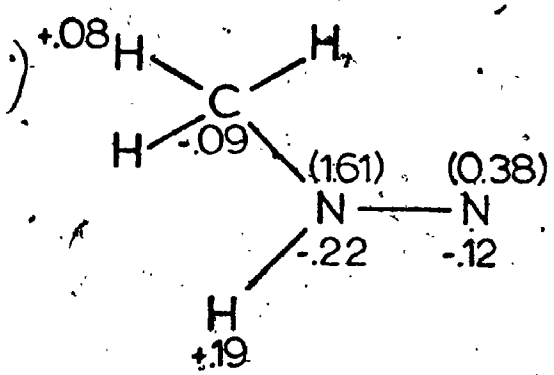

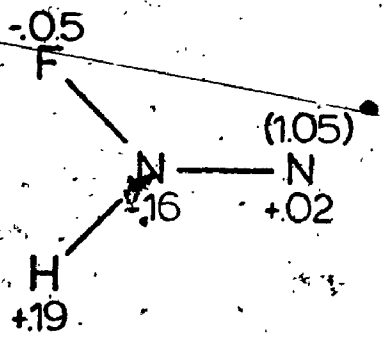

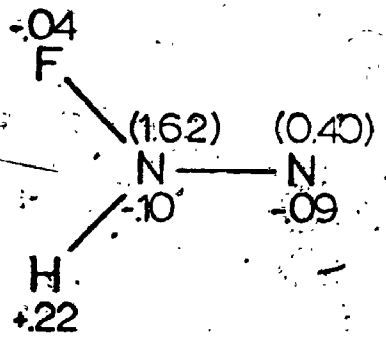

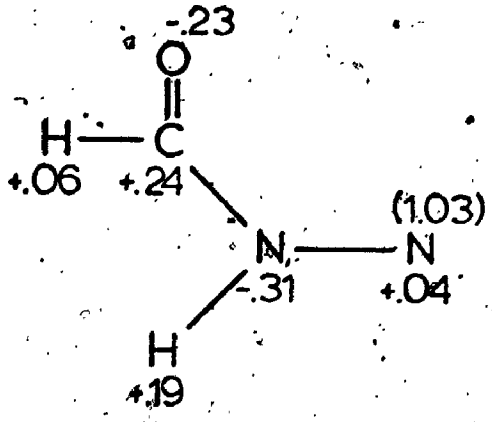

TRIPLET

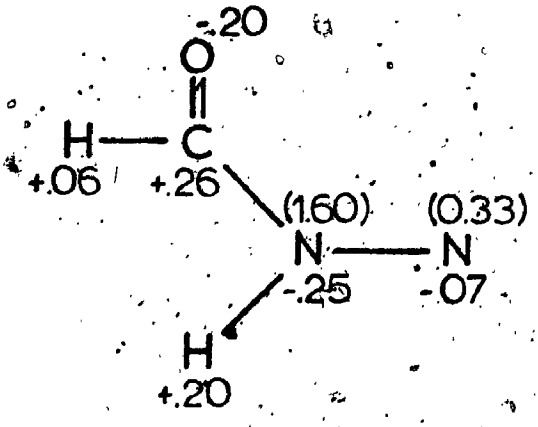

SINGLET

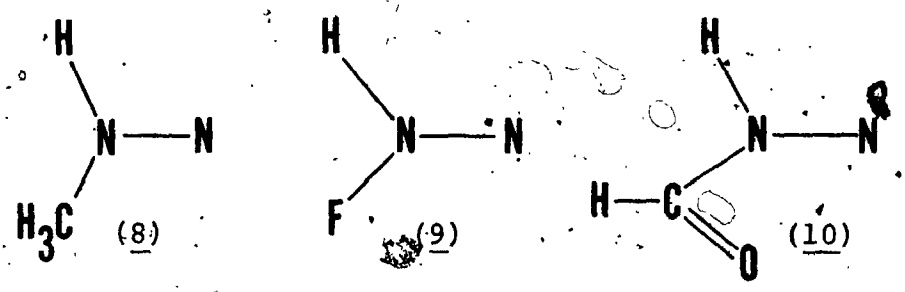

(8) (9) (10)

(9) were taken by analogy with $(CH_3)_3N$ and N_2F_4 (97); C-H distances of 1.089 Å and exactly tetrahedral HCH angles were assumed for the methyl group.

Gross atomic partial charges and selected gross π orbital populations for these derivatives are compared to those for the parent aminonitrene in Figure III-6. Note that the overall effect of each substituent considered, including methyl, is to withdraw electron density from the HNN framework relative to the values calculated for singlet and triplet H_2NN.

The net charge of the nitrene nitrogen is approximately -0.1e in the parent aminonitrene singlet and in all the singlet derivatives considered. Although this amounts to less than half the negative charge predicted by semiempirical calculations, the conclusion by the authors of the latter calculations (91,92) — that the nitrene nitrogen should be nucleophilic — is not altered. For both the methyl and carbonyl derivatives, the changes due to substitution in the net charges on the nitrene nitrogen are almost entirely due to changes in the $2p_\pi$ orbital population (given in parentheses in the diagrams of Figure III-6),

whereas both the σ and π orbital populations of the amino nitrogen are altered. The fluorine atom in (9) donates 0.02e to the NN π electron system, whereas the carbonyl group in (10) withdraws 0.07e; both effects agree qualitatively with intuitive expectations for such substituents. Note, however, that the sum of the π electron density associated with the two nitrogen atoms remains close to 2.0e in all cases.

The changes in the atomic charges due to substitution in the aminonitrene triplet closely parallel those established for the singlets. The total electron density at the amino nitrogen is about 0.07e greater and that for the nitrene nitrogen about 0.11e less in the triplet compared to the singlet in all cases. Note that the nitrene nitrogen is predicted to be electrically neutral in the parent compound.

(e) The Singlet-Triplet Separation and The Ground State of Aminonitrenes

The calculated singlet-triplet separations for each aminonitrene are listed in Table III-17; all values are relative to the singlet at its optimum geometry. The calculated energy separations are interesting in several respects. First, the singlet-triplet separation is quite low and is nowhere near the > 630 kcal mol^{-1} estimate for H_2NN from INDO calculations (91). Second, the triplet at its optimum molecular geometry is predicted to be more stable than the optimum singlet, again in contrast to the

TABLE III-17

Calculated Energies for Aminonitrene Triplets Relative to the Singlet at its Optimum Geometry

Geometry Used for Triplet	Relative Energy (kcal mol^{-1})			
	H_2NN	$CH_3(H)NN$	F(H)NN	HCO(H)NN[a]
Optimum Triplet Geometry	-26.3	-25.7	-24.3	-28.6
Optimum Singlet Geometry	-5.3	-6.0	+3.3	-16.9

[a]The C=O and N=N bonds in HCO(H)NN are assumed to be cis with respect to each other.

semiempirical calculations but in agreement with the ab initio calculations of Wagnière (93). Third, the S_0-T_1 separation is almost zero at the optimum singlet geometry, a prediction which is in good agreement with Wagnière's calculations for which the calculated separation of 2-4 kcal mol^{-1} is for a geometry[1] very close to the optimum singlet structure predicted in the present calculations. Fourth, the singlet-triplet separation is relatively unaffected (within ±3 kcal mol^{-1} when optimum geometries are compared) by substitution. Finally, the calculated separation in H_2NN is approximately 37 kcal mol^{-1} less than that calculated for formylnitrene; a difference which represents the stablization of the singlet state of H_2NN due to delocalization of the amino nitrogen lone pair electrons.

Although the energy separation in H_2NN predicted by the ab initio calculations is expected to be much more realistic than that obtained by semiempirical techniques, there are indications that the values listed in Table III-17 are too negative. In particular, the errors known to be associated with using a minimum basis set of s and p functions to calculate the S_0-T_1, splitting in CH_2 (72,73) (as noted in the previous section in the discussion relating to carbonylnitrenes) also apply to H_2NN. It is anticipated that correction of these errors by carrying out more sophisticated calculations would predict that the optimum triplets

---

[1]Planar with R(NN) = 1.240 Å, R(NH) = 1.021 Å, angle (HNN) = 112°39'.

for aminonitrenes are approximately 10 kcal mol^{-1} more stable than are the optimum singlets, and that in most cases the singlet lies below the triplet at the optimum singlet geometry. Thus the observed chemical reactions of aminonitrenes, all of which have been interpreted as arising from a singlet ground state, may be explicable in terms of a singlet state which undergoes intersystem crossing very slowly to the ground state triplet; i.e., the initially formed aminonitrene becomes "trapped" in the singlet well. Clearly, more refined calculations are needed to settle this important question.

4. The Rotation Barriers in Ethylene and Allene

(a) Introduction

One of the simplest intramolecular chemical reactions is rotation about the double bond in olefins and cummulenes. For appropriately substituted alkenes and planar cummulenes, rotation through the 90° twisted conformation results in interconversion of the cis and trans isomers whereas for the antiplanar members of the cummulene series, rotation through the planar structure can result in optical isomerization.

The desire to accurately predict the activation energy for such reactions has stimulated numerous theoretical studies of the twisting motion in ethylene. Radom and Pople (98), using the STO-3G basis set and the single determinant formalism, calculate a rotation barrier of 138.6 kcal mol^{-1} for ethylene. This value is in reasonable agreement with the single determinant values of 126.1 and 128.9 kcal mol^{-1} obtained by Buenker (99) and by Kaldor and Shavitt (100) respectively, but is in poor agreement with the experimental value of 65 kcal mol^{-1} (101) for the activation energy of the cis, trans isomerization in dideuteroethylene. The principal reason for this large discrepancy between the calculated and experimental barriers arises from the inclusion of "ionic" terms in the single determinant wavefunction. The single configuration ψ_+^2

$$(2+2S_{uv})\psi_+^2 = \{\phi_u(1)\phi_v(2)+\phi_v(1)\phi_u(2)\} + \{\phi_u(1)\phi_u(2)+\phi_v(1)\phi_v(2)\} \quad \text{III-1}$$

is reasonably adequate to describe the bonding between the carbon $2p_\pi$ AOs, ϕ_u and ϕ_v, in the planar ground state of ethylene, but upon rotation away from the planar conformation, the ionic contribution represented by the second term on the right in equation III-1 becomes less and less appropriate to the description of the bonding. Because of this effect, the energy of the single determinant wavefunction rises more rapidly than the true ground state energy. To diminish the importance of the ionic terms, the single configuration, ψ_+^2 must be mixed with the second configuration of the same symmetry, ψ_-^2.

$$(2-2S_{uv})\psi_-^2 = -\{\phi_u(1)\phi_v(2)+\phi_v(1)\phi_u(2)\} + \{\phi_u(1)\phi_u(2)+\phi_v(1)\phi_v(2)\} \quad \text{III-2}$$

In the limit of 90° twisted ethylene, the correct wavefunction is an equal mixture of ψ_+^2 and ψ_-^2 so that the ionic terms cancel and the purely covalent singlet (equation III-3) is recovered.

$$2^{-\frac{1}{2}}(\psi_+^2 - \psi_-^2) = 2^{-\frac{1}{2}}\{\phi_u(1)\phi_v(2) + \phi_v(1)\phi_u(2)\} \quad \text{III-3}$$

When Buenker (99) and Kaldor and Shavitt (100) include this configuration interaction in their calculations, a substantial lowering in the barrier height to 83.7 and 83.3 kcal mol^{-1} respectively, is obtained. Buenker, Peyerimhoff and Hsu (38), using a large Gaussian basis set and more than the minimum CI, have shown that a further improvement in the calculated barrier height can be achieved by optimizing

the carbon-carbon bond length in both the planar and twisted conformations. In particular, it has been found that a substantial lengthening of this bond from 1.33 Å predicted for the planar ground state to 1.47 Å for the 90° twisted species leads to a predicted barrier height of 63.7 kcal mol^{-1}, in good agreement with the experimental value. The most recent calculation, reported by Wood (102), employs Double Configuration (DC) SCF methods coupled with bond length optimization and leads to a calculated activation energy of 63.2 kcal mol^{-1} for the ethylene cis, trans isomerization.

In contrast to the results for ethylene, the results of calculations on the barrier height in allene are not nearly so satisfying. Unfortunately, no experimental estimate is available for this barrier, but since the hydrogen atoms are further apart in allene than in ethylene, it might be intuitively expected that the rotation barrier in allene would be lower than that in ethylene. Schaad (103) has shown that the use of simple Huckel theory, parametrized to reproduce the experimental ethylene barrier, leads to a value of 38 kcal mol^{-1} for the allene barrier. However, a variety of ab initio SCF calculations have recently been reported in which the predicted barrier for allene is higher than that for ethylene. Calculations by Radom and Pople (98), Schaad, Burnelle and Dressler (104), André and coworkers (105), Preuss and Janoschek (106), Buenker (99), and Weimann and Christoffersen (107) predict values which are, respectively, 91.9, 72.7, 74.6, 65, 82.1, and 75.1 kcal mol^{-1}. Although these predictions are all in reasonable

agreement with one another, none of the above calculations properly describes the planar conformation of allene. Rotation to the planar form involves breaking one of the two quasi-localized π bonds (see Figure III-7) in the same way that the rotation in ethylene destroys the single π bond. However, in allene the $2p_\pi$ orbital on the end carbon atom is rotated into line with the remaining π bond and becomes part of the $1b_{2g}$ nonbonding MO in D_{2h} symmetry. This latter interaction stablizes this MO while the other $2p_\pi$ AO on the central carbon in the plane of the molecule becomes the nonbonding $2b_{2u}$ MO. Thus the degeneracy which occurs in ethylene does not materialize in allene and CI treatments for the lowest singlet state are not of the same importance. In the terminology of Salem and Rowland (108), planar allene is a "heterosymmetric" diradical (i.e., the two electrons responsible for the diradical behaviour occupy non-equivalent, non-degenerate MOs). The correct description of the lowest singlet of this species is by the open-shell configuration ^1A_u, in which each of the $1b_{2g}$ and $2b_{2u}$ MOs are singly-occupied. Twisted ethylene, on the other hand, is a "homosymmetric" diradical (i.e., the two electrons are equivalent and occupy degenerate MOs) which is properly described as a mixture of two closed-shell configurations. All of the above mentioned calculations for planar allene converge to the ^1A_g state corresponding to a doubly-occupied $1b_{2g}$ MO and a vacant $2b_{2u}$ MO. Buenker (99) has shown that attempts to improve the energy of the lower

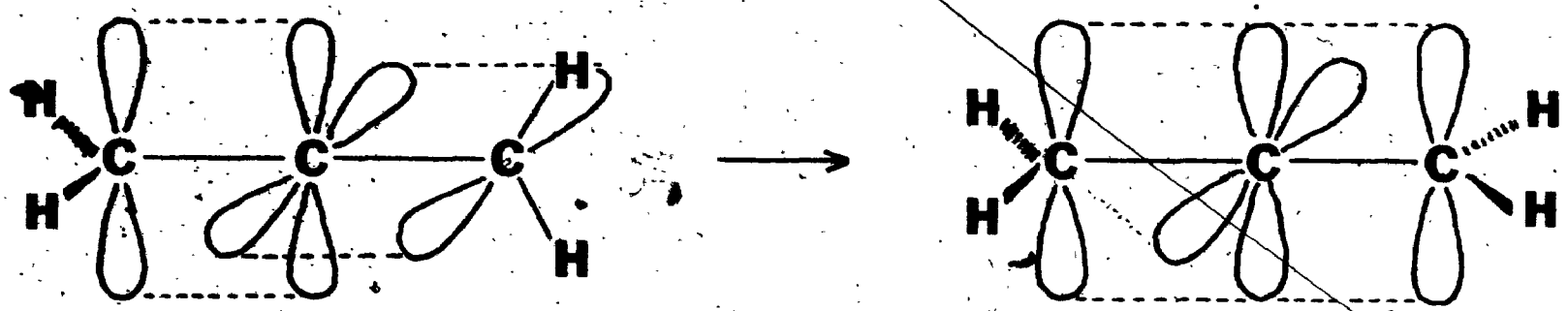

FIGURE III-7

Localized Orbital Model of Allene Rotation

^1A_g state by including CI with the second ^1A_g state (formed by doubly occupying the $2b_{2u}$ MO rather than $1b_{2g}$) lead to a negligible energy lowering of 1×10^{-4} a.u., i.e., less than 0.1 kcal mol^{-1}. Although Schaad, Burnelle and Dressler (104) calculate the energy of the ^1A_u state using the orbitals determined for the ^1A_g state, they find that the energy of this state is only 0.7 kcal mol^{-1} lower than that of ^1A_g. This small difference is not surprising since the $1b_{2g}$ orbital is formally the non-bonding "allyl" orbital localized on the end carbon atoms, while the $2b_{2u}$ orbital is localized on the central carbon. Thus excitation between these two orbitals in going from the ^1A_g to the ^1A_u states involves a significant amount of charge transfer and consequently the use of closed-shell eigenvectors is expected to lead to a significant error.

The motivation for the present research was first the desire to show that the minimal STO-3G basis set was appropriate for the calculation of double bond barrier heights, and second to confirm the simple intuitive prediction of a lower barrier in allene than in ethylene. Thus, in the next section, the results of STO-3G calculations including both 2X2 CI and geometry optimization, are presented for planar and 90° twisted ethylene. In the final section SCF results using the Roothaan open-shell method are presented for the twisted and planar conformations of allene.

(b) Ethylene

In order to effectively assess the performance of the

STO-3G basis set in calculating rotational barriers, the ethylene calculations were carried out in two stages. First the effect of CI was considered by carrying out calculations on the planar and 90° twisted conformations using bond lengths and angles, determined by the STO-3G single-determinant method (15) to be optimum for the planar species (i.e., R(CC) = 1.306 Å, R(CH) = 1.082 Å and angle (HCH) = 115.6°). Employing simple 2X2 CI for both conformations leads to a differential lowering of 44.1 kcal mol^{-1} in the energy of the twisted conformation so that the barrier is predicted to 94.5 kcal mol^{-1} rather than the value of 138.6 kcal mol^{-1} calculated by Radom and Pople using the STO-3G basis set (98). An improvement of this magnitude agrees well with the CI improvements of 42.4 and 45.6 kcal mol^{-1} found by Buenker (99) and by Kaldor and Shavitt (100), respectively. Second, optimization of the C-C bond length was carried out using the same C-H bond lengths and HCH bond angles as before. Inclusion of CI in this procedure leads to a C-C bond length in the planar species of 1.34 Å, which is in much better agreement with the experimental value of 1.338 Å (109) than is the single determinant value, and to a C-C bond length of 1.498 Å for the 90° twisted conformation. Total CI energies for the planar and twisted conformations are calculated to be -77.11681 and -77.00099 a.u., respectively, yielding a barrier height of 72.7 kcal mol^{-1}. Although this value is somewhat higher than the experimental value, the improvement in the calculated barrier

achieved by varying the C-C bond distance agrees well with that found by Buenker, Peyerimhoff and Hsu (38). A further lowering can be achieved by optimization of the exponents of the carbon $2p_\pi$ orbitals. In particular, employing the optimum value of 1.52 found for these orbitals in the planar conformation, 1.48 found for the 90° twisted species and standard exponents for all other orbitals yields a barrier of 69.4 kcal mol^{-1}. In general, therefore, it can be concluded that the use of the STO-3G basis set with standard exponents leads to double bond rotation barriers which are only slightly overestimated.

(c) Allene

As discussed above, the wavefunction for the anti-planar ground state of allene undergoes a change in character upon rotation to a planar geometry. In particular, the lowest singlet state of the twisted conformation, ($^1A_1$ in D_{2d} symmetry) which is described by a closed-shell electron configuration, correlates with the open-shell singlet, ^1A_u in D_{2h} symmetry. Direct calculation of the ^1A_u wavefunction (and hence the energy) is, however, not possible with Roothaan's open-shell formalism. In the present calculations, the ^1A_u energy is calculated from the optimum ^3A_u wavefunction which is calculated by the open-shell method. This approximation is not expected to be severe for planar allene since the electron distribution should be almost identical in both the ^1A_u and ^3A_u states. In addition, the exchange integral between the singly-occupied orbitals,

$1b_{2g}$ and $2b_{2u}$, is calculated to be only 0.00082 a.u. so that any difference between the ^1A_u and ^3A_u wavefunctions due to the interaction of the unpaired electrons should be small. For the $^1A_1$ state of twisted allene, 2X2 CI has been included in the calculation of the energy to compensate for the electron correlation introduced in the ^1A_u state by the use of open-shell procedures. That is, the motions of the two electrons in singly-occupied orbitals in ^1A_u are automatically correlated since they occupy different spatial orbitals, so CI must be included in the calculation of the $^1A_1$ energy if the two conformations are to be treated equally.

Using C-H bond lengths of 1.083 Å and HCH angles of 116.2°, (as calculated by Pople and co-workers (16) in single determinant STO-3G calculations) optimization of the C-C bond lengths in the twisted $^1A_1$ state yields a value of 1.30 Å, in good agreement with the experimental estimate of 1.308 Å (110). The total CI energy for this geometry is calculated to be -114.4336 a.u.. For the ^1A_u state of planar allene, the C-C bonds are predicted by the present calculations to lengthen to 1.34 Å. Note that the lengthening in allene accompanying the rupture of a π bond is not nearly so dramatic as that in ethylene, since in planar allene, the C-C linkages retain some multiple bonding character. The total energy for the planar conformation is calculated to be -114.34515 a.u., or 55.5 kcal mol^{-1} higher than that calculated for the twisted species. Thus the

barrier to rotation in allene is predicted to be 17.2 kcal mol^{-1} lower than that predicted for ethylene, in agreement with intuitive expectations. Although this barrier height is probably overestimated with the STO-3G basis set, it is anticipated that the difference between the allene and ethylene values is closely reproduced.

5. Ethylenedione

(a) Introduction

Recently some attention, both of a theoretical and of an experimental nature, has been paid to ethylenedione, O=C=C=O. This molecule is interesting in at least two respects; first, it is the lowest even-carbon member of the oxycummulene series, $O=C_n=O$, which by analogy with the odd-carbon series should be most stable. Second, simple qualitative MO arguments (111) indicate that the ground state of C_2O_2 is a triplet state with an electronic structure analogous with that of O_2 or NCN.

Experimentally, C_2O_2 has eluded detection, presumably because dissociation to two molecules of C≡O is a facile process. The positive ion, $C_2O_2^+$, has however been observed in mass spectral studies (112) and the neutral fragment, C_2O_2 is apparently expelled intact from α,β-unsaturated-γ-dilactones in the mass spectra of these compounds (113). In addition, C_2O_2 has been postulated as a stable intermediate in the chemiluminescence reactions of hydrocarbon-oxygen flames. Direct attempts to synthesize ethylenedione have involved the pyrolysis and photolysis of annelated derivatives of bicyclo(2.2.2)octadiene-2,3-dione (1), but for

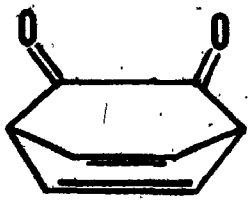

(1)

both reactions the observed product was carbon monoxide

rather than ethylenedione (114-116). This latter observation is particularly puzzling given that the expulsion of C_2O_2 from (1) is formally a disrotatory reverse 2+4 cycloaddition and thus is thermally allowed by orbital symmetry rules (117). In addition, the corresponding monoketones fragment readily to yield ketene and aromatic hydrocarbons (118).

The qualitative prediction of a triplet ground state for ethylenedione has been supported by both semiempirical and ab initio calculations. In particular, calculations employing the INDO method (119,120) have predicted a linear, triplet ground state which is bound with respect to two CO molecules. Ab initio calculations reported by Beebe and Sabin (121) predict that the lowest-energy linear conformation of C_2O_2 is ≈2.4eV (65.3 kcal mol^{-1}) lower in energy than two isolated CO molecules and that singlet states of Δ_g and Σ_g^+ symmetry lie 29.4 and 61.8 kcal mol^{-1} respectively, above the $^3\Sigma_g^-$ ground state. The potential curves for all three of these low-lying states are predicted to have minima for a C-C bond length in the neighbourhood of 1.34 Å and are predicted to dissociate to products not corresponding to ground state CO molecules.

Thus, theoretical predictions suggest that ethylenedione is stable with respect to two CO molecules and indicate that it should be observable provided it is prepared under appropriate reaction conditions. The calculations reported here were undertaken in order to investigate the

apparent dichotomy between the experimental results and the theoretical predictions. In particular, it is of interest to confirm the results of the calculations reported by Beebe and Sabin by reexamining the electronic structure of ethylenedione, and to determine the reasons for the failure in the synthesis of C_2O_2 from the diones represented by (1).

(b) Results and Discussion

The lowest energy states of linear O=C=C=O, $^3\Sigma_g^-$, $^1\Delta_g$ and $^1\Sigma_g^+$, are derived from the open-shell electron configuration, (core) $1\pi_u^4\ 1\pi_g^4\ 2\pi_u^2$. According to Hund's rule, the triplet state of this configuration lies lowest in energy, and the $^1\Sigma_g^+$ state highest in energy. Although Roothaan's open-shell method is formally capable of treating all three states directly, convergence problems were encountered for the two singlet states. For this reason, the optimum wavefunction obtained for the triplet state was used to describe the singlet states in the present calculations. Computation of the energy for these singlet states is achieved by taking linear combinations of the two determinants formed by doubly occupying in turn, each component of the $2\pi_u$ MO. The error introduced by so doing is not expected to be appreciable since the electron configuration is the same for all three states.

Using this technique with the STO-3G basis set, C_2O_2 is predicted to be bound in all three of its low-lying

states; optimum C=C and C=O bond lengths for the linear conformation are listed in Table III-18. It should be noted that the predicted C=C bond lengths for the three states are somewhat shorter than both the values predicted by Beebe and Sabin (121) (1.335, 1.350 and 1.350 Å for $^3\Sigma_g^-$, $^1\Delta_g$ and $^1\Sigma_g^+$, respectively), and the value of ≈1.34 Å usually expected for ethylenic C=C double bonds (122). The C=O bonds, on the other hand, are predicted to be longer than the value of 1.162 Å found experimentally for CO_2 (33). In addition, the total calculated C=C and C=O overlap populations of 1.294 and 0.870e respectively, are consistent with a classical cummulene structure. The gross orbital and atomic populations listed in Table III-19 for the $^3\Sigma_g^-$ state indicate a slight polarization of the σ electrons toward the oxygen atoms, resulting in a charge distribution with like charges on the adjacent carbon atoms.

The total STO-3G energy for the $^3\Sigma_g^-$ state at its optimum geometry is calculated to be -222.35175 a.u.. The minimum energy $^1\Delta_g$ and $^1\Sigma_g^+$ states are predicted to lie 17.0 and 34.0 kcal mol^{-1} above the triplet state. These energies can be compared to a total energy of -222.45086 a.u. for two isolated molecules of carbon monoxide (each calculated at the predicted optimum C≡O bond length of 1.145 Å). Thus, in contrast to the calculations by Beebe and Sabin, the STO-3G calculations predict that C_2O_2 is 62.2 kcal mol^{-1} less stable than two molecules of C≡O. The reason for this rather large discrepancy between the two ab initio calcula-

TABLE III-18

Calculated Optimum Bond Lengths (in Å) for the Three Lowest States of Linear C_2O_2

State	R(CC)	R(CO)
$^3\Sigma_g^-$	1.263	1.207
$^1\Delta_g$	1.268	1.209
$^1\Sigma_g^+$	1.272	1.209

TABLE III-19

Gross Orbital Populations for the $^3\Sigma_g^-$ State of C_2O_2

Atom	Orbital[a]	Population (in e)
C	1s	1.9943
	2s	0.9793
	$2p_x = 2p_y$	0.9994
	$2p_z$	0.8842
	total atomic	5.8566
O	1s	1.9980
	2s	1.8667
	$2p_x = 2p_y$	1.5006
	$2p_z$	1.2775
	total atomic	8.1434

[a]The coordinate system was chosen with the z axis coincident with the molecular axis.

tions is not immediately obvious, but it should be pointed out that the STO-3G energy for C_2O_2 leads to an atomization energy in reasonable agreement with empirical expectations. In particular, subtraction of the optimum STO-3G atom energies, calculated by Pople and co-workers (10), from the total C_2O_2 $^3\Sigma_g^-$ energy results in an atomization energy of 0.28593 a.u. which is 0.05844 a.u. greater than the atomization energy calculated for CO_2 (10;19). Given that the single determinant approximation generally greatly underestimates bonding energy and that the C=O bonds in CO_2 are likely somewhat stronger than in C_2O_2 (the C=O bond distance is somewhat shorter in CO_2), this estimate of 36.6 kcal mol^{-1} for the C=C bond energy in C_2O_2 indicates that the present calculations give a reasonable result. In addition, the singlet-triplet separations of 17 and 34 kcal mol^{-1} calculated herein are more in line with chemical intuition than are the values of 29.4 and 61.8 kcal mol^{-1} calculated by Beebe and Sabin. Specifically, the electronic structure of C_2O_2 is similar to that of O_2 for which the $^3\Sigma_g^- - ^1\Delta_g$ and $^3\Sigma_g^- - ^1\Sigma_g^+$ separations are found experimentally to be 22.6 and 37.6 kcal mol^{-1} respectively (123). Since, in C_2O_2, the unpaired electrons responsible for the separations are, on the average, further apart than in O_2, the singlet-triplet separations should be smaller in C_2O_2 than in O_2. In summary, the present calculations indicate that the dissociation of ethylenedione to two molecules of C≡O is, overall, an exothermic process,

but the prediction of a stable minimum for C_2O_2 by both the present calculations and those of Beebe and Sabin, suggests that, under the proper conditions, it should be a detectable species.

As pointed out earlier, attempts to synthesize C_2O_2 by pyrolysis and photolysis of 1,2-diones have met with failure. Several reasons may be suggested for this lack of success, the foremost of which is that the C_2O_2 initially produced, subsequently dissociates to CO and thus goes undetected. This, however, seems unlikely in view of the results presented above. Alternatively, the stepwise loss of CO, rather than the concerted loss of C_2O_2 from the dione, is a possible pathway, but this also seems unlikely given that the corresponding monoketones extrude ketene readily (118), and that the concerted loss of C_2O_2 is a symmetry-allowed reaction (117). In addition, the arguments presented by Haddon (119), that the triplet-singlet separation in C_2O_2 is sufficiently large to prevent the formation of the allowed $^1\Delta_g$ product, are not plausible given that analogous reactions of peroxides are known to produce O_2 in the $^1\Delta_g$ state (124).

It is instructive to note that the geometrical configuration of the dione unit is somewhat removed from that of stable linear ethylenedione. In particular, the CCO angle in the dione is approximately 120° and the C-C bond distance is expected to be substantially longer than the C=C bond distance in C_2O_2. Thus the ethylenedione produced

initially will be considerably distorted from its equilibrium geometry. To investigate the effects of this distortion on the electronic structure of C_2O_2, STO-3G calculations have been carried out for several different CCO angles. Cis-bending of the molecule at the carbon atoms, lifts the degeneracy of the π orbitals so that the highest occupied MO of the linear conformation, $2\pi_u$, splits into two components of a_1 and b_1 symmetry in the C_{2v} point group. One of these two orbitals, the a_1 orbital, is destablized on bending so that the lowest closed-shell singlet of the bent molecule corresponds to a double occupation of the π type, b_1 orbital. For small CCO angles the triplet state corresponding to singly-occupied a_1 and b_1 orbitals is the ground state, but before the CCO angle reaches 130°, the $^1A_1$ state becomes the ground state. The destablization of the a_1 orbital is also reflected by an increase in the optimum C-C bond distance; at an angle of 130°, the optimum value is found to be 1.313 Å corresponding to a total (single determinant) energy of -222.23097 a.u. or 75.8 kcal mol^{-1} above that of the optimum linear triplet. Corresponding to the destablization of the a_1 orbital, stablization of an orbital of b_2 symmetry, derived from the (vacant) $2\pi_g$ MO of the linear conformation, also accompanies the bending (see Figure III-8). At a CCO angle of 110°, double occupation of this b_2 orbital becomes energetically more favourable than double occupation of the b_1 orbital so that the lowest energy $^1A_1$ state of the 110° bent conformation corresponds

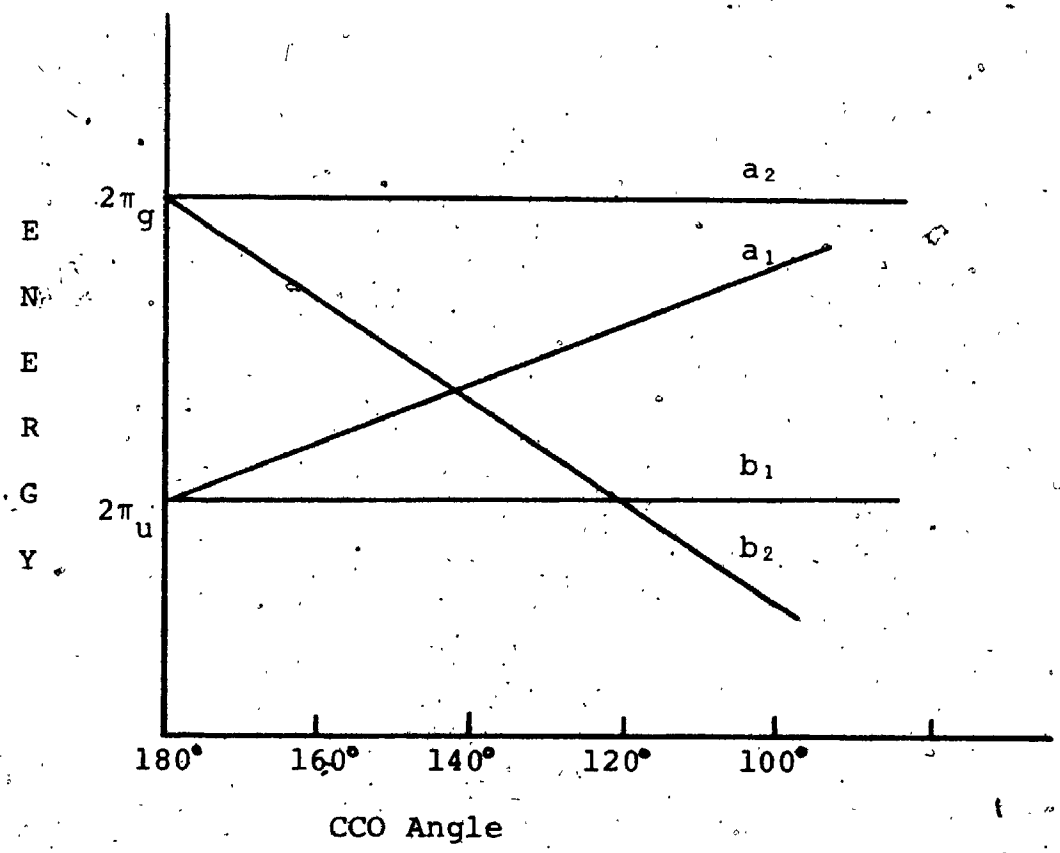

FIGURE III-8

Schematic Illustration of the Orbital Energy Variation Accompanying Cis-Bending in C_2O_2

to a different electron configuration than does the lowest singlet state of the 130° bent conformation. That is, at an angle intermediate between 130° and 110°, the b_1 and b_2 orbitals become degenerate and an avoided crossing of two states of $^1A_1$ symmetry occurs. The lowest energy $^1A_1$ state of the 110° bent species however, correlates smoothly with two ground state CO molecules. Gradual lengthening of the CC distance for this configuration is accompanied by a sharp drop in the total energy so that for distances in excess of 1.80 Å, the total C_2O_2 energy is less than that of the bound linear conformation.

Thus, in disagreement with orbital symmetry rules, production of C_2O_2 from 1,2-diones is likely to lead to two molecules of C≡O, because the initially expelled fragment is formed in a region of the potential surface where dissociation to C≡O is the energetically more facile pathway. For this reason, 1,2-diones are not expected to be precursors for C_2O_2 so that if this molecule is to be studied experimentally in any detail, an alternative synthesis must be found.

REFERENCES

1. F. Hund, Z. Physik, 40, 742 (1927); 42, 93 (1927); 63, 719 (1930).

2. R.S. Mulliken, Phys. Rev., 32, 186 (1928); Rev. Mod. Phys., 2, 60 (1930); 3, 89 (1931); 4, 1 (1932).

3. J.E. Lennard-Jones, Trans. Faraday Soc., 25, 668 (1929).

4. E. Huckel, Z. Physik, 70, 204 (1931); 72, 310 (1931); 76, 628 (1932).

5. B.J. Ransil, Rev. Mod. Phys., 32, 239, 245 (1960).

6. L. Radom, "A Bibliography of Ab Initio Molecular Orbital Calculations", Carnegie-Mellon University, Pittsburg, Pa. (1972). (unpublished)

7. C.C.J. Roothaan, Rev. Mod. Phys., 23, 69 (1951).

8. C.C.J. Roothaan, Rev. Mod. Phys., 32, 179 (1960).

9. S.F. Boys, Proc. Roy. Soc. (London), A200, 542 (1950).

10. W.J. Hehre, R.F. Stewart and J.A. Pople, J. Chem. Phys., 51, 2657 (1969).

11. W.J. Hehre, R. Ditchfield, R.F. Stewart and J.A. Pople, J. Chem. Phys., 52, 2769 (1970).

12. I.G. Csizmadia, M.C. Harrison, J.W. Moskowitz and B.T. Sutcliffe, Theoret. Chim. Acta, 6, 191 (1966).

13. E. Clementi and D.R. Davis, J. Comput. Phys. 2, 223 (1967).

14. R.D. Newton, W.A. Lathan, W.J. Hehre and J.A. Pople, J. Chem. Phys., 52, 4064 (1970).

15. W.A. Lathan, W.J. Hehre and J.A. Pople, J. Amer. Chem. Soc., 93, 808 (1971).

16. L. Radom, W.A. Lathan, W.J. Hehre and J.A. Pople, J. Amer. Chem. Soc., 93, 5339 (1971).

17. W.A. Lathan, W.J. Hehre, L.A. Curtiss and J.A. Pople, J. Amer. Chem. Soc., 93, 6377 (1971).

18. W.J. Hehre and J.A. Pople, J. Amer. Chem. Soc., 92, 2191 (1970).

19. W.J. Hehre, R. Ditchfield, L. Radom and J.A. Pople, J. Amer. Chem. Soc., 92, 4796 (1970).

20. R. Ditchfield, W.J. Hehre and J.A. Pople, J. Chem. Phys., 54, 724 (1971).

21. R.S. Mulliken, J. Chem. Phys., 23, 1833, 1841, 2338, 2343 (1955).

22. F.L. Pilar, "Elementary Quantum Chemistry", McGraw-Hill, New York, 1968, pp. 364-365.

23. J.A. Pople and R.K. Nesbet, J. Chem. Phys., 22, 571 (1954).

24. R.K. Nesbet, Proc. Roy. Soc. (London), A230, 312 (1955).

25. W.J. Hunt, T.H. Dunning and W.A. Goddard, Chem. Phys. Lett., 3, 606 (1969).

26. G.A. Segal, J. Chem. Phys., 53, 360 (1970).

27. D.H. Sleeman, Theoret. Chim. Acta, 11, 135 (1968).

28. M.J.S. Dewar, J.A. Hashmall and C.G. Venier, J. Amer. Chem. Soc., 90, 1953 (1968).

29. M.J.S. Dewar and N. Trinajstic, Chem. Commun., 646 (1970).

30. G. Diercksen, Int. J. Quant. Chem., 2, 55 (1967).

31. H.C. Longuet-Higgins and J.A. Pople, Proc. Physical Soc., A68, 591 (1955).

32. P. Carsky and R. Zahradnik, Theoret. Chim. Acta, 26, 171 (1972).

33. G. Herzberg, "Molecular Spectra and Molecular Structure", Vol. III, Van Nostrand, Princeton, N.J., 1967.

34. N.C. Baird, unpublished STO-3G calculations.

35. A.W. Salofte and L. Burnelle, J. Chem. Phys., 53, 333 (1970).

36. S.V. O'Neill, H.F. Schaeffer and C.F. Bender, J. Chem. Phys., 55, 162 (1971).

37. R. Ditchfield, J. Del Bene and J.A. Pople, J. Amer. Chem. Soc., 94, 4806 (1972).

38. R.J. Buenker, S.D. Peyerimhoff and H.L. Hsu, Chem. Phys. Lett., 11, 65 (1971).

39. A. Almenningen, O. Bastiansen and M. Traetteberg, Acta Chem. Scand., 12, 1221 (1958).

40. C.W. Mathews, Can. J. Phys., 45, 2355 (1967).

41. V. Menendes and J.M. Figuera, Chem. Phys. Lett., 18, 426 (1973).

42. N.C. Baird and J.R. Swenson, Can. J. Chem., 51, 3097 (1973).

43. R. Macauley, L.A. Burnelle and C. Sandorfy, Theoret. Chim. Acta, 29, 1 (1973).

44. N.C. Baird and R.F. Barr, Can. J. Chem., 51, 3303 (1973).

45. N.C. Baird and J.R. Swenson, J. Phys. Chem., 77, 277 (1973).

46. P.J. Hay and W.A. Goddard, Chem. Phys. Lett., 14, 46 (1972).

47. G.E. Coates and K. Wade, "Organometallic Compounds", 3rd ed., Vol. 1, Methuen, London, 1967, p.103.

48. N.R. Fetter, Organometal. Chem. Rev., 3, 1 (1968).

49. G.E. Coates and G.L. Morgan, Advan. Organometal. Chem., 9, 195 (1970).

50. K. Ohkubo, H. Shimada and M. Okada, Bull. Chem. Soc. Japan, 44, 2025 (1971).

51. R.A. Kovar and G.L. Morgan, Inorg. Chem., 8, 1099 (1969).

52. T.L. Brown, Advan. Organometal. Chem., 3, 365 (1965).

53. H.L. Lewis and T.L. Brown, J. Amer. Chem. Soc., 92, 4664 (1970).

54. A.I. Snow and R.E. Rundle, Acta Crystallogr., 4, 348 (1951).

55. G.E. Coates and P.D. Roberts, J. Chem. Soc., A, 2651 (1968).

56. A. Almenningen, A. Haaland and G.L. Morgan, Acta Chem. Scand., 23, 2921 (1969).

57. M.J.S. Dewar, "Hyperconjugation", Ronald Press, New York, 1962.

58. E. Clementi and D.L. Raimondi, J. Chem. Phys., 51, 2657 (1963).

59. A. Almenningen, A. Haaland and J.E. Nilsonn, Acta Chem. Scand., 22, 972 (1968).

60. N.C. Baird, R.F. Barr and R.K. Datta, J. Organometal. Chem., 59, 65 (1973).

61. R. Ahlrichs, Theoret. Chim. Acta, 17, 348 (1970).

62. A.H. Clark and A. Haaland, Chem. Commun., 912 (1969).

63. J.L. Atwood and G.D. Stucky, Chem. Commun., 1169 (1967); J. Amer. Chem. Soc., 91, 4426 (1969).

64. W. Lwowski, Ed., "Nitrenes", Wiley-Interscience, New York, 1970.

65. W. Kirmse, "Carbene Chemistry", 2nd edition, Academic Press, New York, 1971.

66. J.S. McConaghy and W. Lwowski, J. Amer. Chem. Soc., 89, 2357, 4450 (1967).

67. P.S. Skell and R.C. Woodworth, J. Amer. Chem. Soc., 78, 4496 (1956).

68. E. Wasserman, Progr. Phys. Org. Chem., 8, 319 (1971).

69. R.S. Berry, reference 64, pp. 45-46.

70. G. Just and W. Zehetner, Tetrahedron Lett., 3389 (1967).

71. P.F. Alewood, P.M. Kazmaier and A. Rauk, J. Amer. Chem. Soc., 95, 5466 (1973).

72. H.F. Schaeffer III, "The Electronic Structure of Atoms and Molecules", Addison-Wesley, 1972, pp. 309-316.

73. C.F. Bender, H.F. Schaeffer III, D.R. Francesschetti and L.C. Allen, J. Amer. Chem. Soc., 94, 6888 (1972).

74. P.J. Hay, W.J. Hunt and W.A. Goddard III, Chem. Phys. Lett., 13, 30 (1972).

75. V. Staemmler, Theoret. Chim. Acta, 31, 49 (1973).

76. H.M. Frey, J. C. S. Chem. Commun., 1024 (1972).

77. W.L. Hase, R.J. Phillips and J.W. Simons, Chem. Phys. Lett., 12, 161 (1971).

78. W.J. Haines and I.G. Csizmadia, Theoret. Chim. Acta, 31, 283 (1973).

79. R. Hoffmann, J. Amer. Chem. Soc., 90, 1475 (1968).

80. I.L. Karle and J. Karle, J. Chem. Phys., 22, 43 (1954).

81. P.C. Hariharan and J.A. Pople, Chem. Phys. Lett., 16, 217 (1972).

82. S.P. McGlynn, T. Azumi and M. Kinoshita, "Molecular Spectroscopy of the Triplet State", Prentice-Hall Inc., Englewood Cliffs, N.J., 1969, pp. 13-17.

83. B.V. Ioffe and M.A. Kuznetzov, Russ. Chem. Revs., 41, 131 (1972).

84. D.M. Lemal, reference 64, pp. 345-404.

85. R.S. Atkinson and C.W. Rees, Chem. Commun., 1230 (1967).

86. D.J. Anderson, T.L. Gilchrist, D.C. Horwell and C.W. Rees, Chem. Commun., 146 (1969).

87. D.J. Anderson, T.L. Gilchrist and C.W. Rees, Chem. Commun., 147 (1969).

88. R.S. Atkinson and C.W. Rees, J. Chem. Soc. (C), 772 (1969).

89. D.J. Anderson, T.L. Gilchrist, D.C. Horwell and C.W. Rees, J. Chem. Soc. (C), 576 (1970).

90. M. Bandru and A. Foucaud, Comptes Rendu., 270, 104 (1970).

91. L.J. Hayes, F.P. Billingsley II and C. Trindle, J. Org. Chem., 37, 3924 (1972).

92. Y.A. Bespalov, L.A. Kartsova, V.I. Baranovski and B.V. Ioffe, Dokl. Akad. Nauk SSSR, 200, 99 (1971).

93. G. Wagnière, Theoret. Chim. Acta, 31, 269 (1973).

94. D. Pan Wong, W.H. Fink and L.C. Allen, J. Chem. Phys., 52, 6291 (1970).

95. N.C. Baird and R.K. Datta, Inorg. Chem., 11, 17 (1972).

96. C.C. Costain and J.M. Dowling, J. Chem. Phys., 32, 158 (1960).

97. L.E. Sutton, Ed., "Tables of Interatomic Distances and Configurations in Molecules and Ions", Special Publications 11 and 18, The Chemical Society, London, 1959 and 1965.

98. L. Radom and J.A. Pople, J. Amer. Chem. Soc., 92, 4786 (1970).

99. R.J. Buenker, J. Chem. Phys., 48, 1368 (1968).

100. U. Kaldor and I. Shavitt, J. Chem Phys., 48, 191 (1968).

101. J.E. Douglas, B.S. Rabinovitch and F.S. Looney, J. Chem. Phys., 23, 315 (1955).

102. M.H. Wood, Chem. Phys. Lett., 24, 239 (1974).

103. L.J. Schaad, Tetrahedron, 26, 4115 (1970).

104. L.J. Schaad, L.A. Burnelle and K.P. Dressler, Theoret. Chim. Acta, 15, 91 (1969).

105. J.-M. André, M.-C. André and G. Leroy, Chem. Phys. Lett., 3, 695 (1969).

106. H. Preuss and R. Janoschek, J. Mol. Struct., 3, 423 (1969).

107. L.J. Seimann and R.E. Christoffersen, J. Amer. Chem. Soc., 95, 2074 (1973).

108. L. Salem and C. Rowland, Angew. Chem. Internat. Edit., 11, 92 (1972).

109. A.J. Merer and R.S. Mulliken, Chem. Rev., 69, 639 (1969).

110. A.G. Maki and R.A. Toth, J. Mol. Spectry., 17, 136 (1965).

111. D.M. Hirst, J.D. Hopton and J.W. Linnett, Tetrahedron, 19, Suppl. 2, 15 (1963).

112. M. Saporoschenko, J. Chem. Phys., 49, 768 (1968).

113. P. Kolsaker, Org. Mass Spectrom., 7, 535 (1973).

114. J. Strating, B. Zwanenburg, A. Wagenaar and A.C. Udding, Tetrahedron Lett., 125 (1968).

115. D. Bryce-Smith and A. Gilbert, Chem. Commun., 1702 (1968).

116. D.L. Dean and H. Hart, J. Amer. Chem. Soc., 94, 687 (1972).

117. R.B. Woodward and R. Hoffmann, "The Conservation of Orbital Symmetry", Verlag Chemie, Weinheim, Germany, 1970.

118. R.K. Murray, Jr. and H. Hart, Tetrahedron Lett., 4995 (1968).

119. R.C. Haddon, Tetrahedron Lett., 3897 (1972).

120. P. Lindner, Y. Ohrn and J.R. Sabin, Int. J. of Quantum Chem. Symp., 7, 261 (1973).

121. N.H.F. Beebe and J.R. Sabin, Chem. Phys. Lett., 24, 389 (1974).

122. L. Pauling, "The Nature of the Chemical Bond", 3rd ed., Cornell University Press, Ithaca, N.Y., 1960.

123. G. Herzberg, "Molecular Spectra and Molecular Structure" Vol. II, Van Nostrand, Princeton, N.J., 1950.

124. D.R. Kearns, J. Amer. Chem. Soc., 91, 6554 (1969).